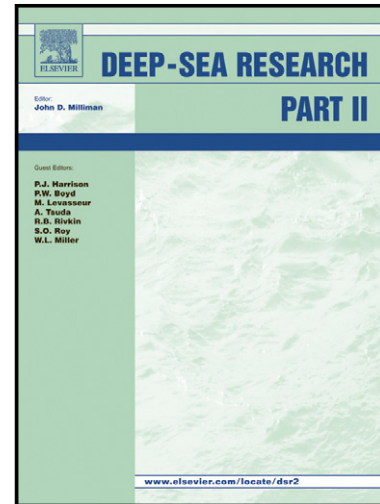


Author's Accepted Manuscript

Surface nitrate utilization in the Bering sea since 180 kA BP: Insight from sedimentary nitrogen isotopes

Jan-Rainer Riethdorf, Benoit Thibodeau, Minoru Ikehara, Dirk Nürnberg, Lars Max, Ralf Tiedemann, Yusuke Yokoyama



www.elsevier.com/locate/dsr2

PII: S0967-0645(15)00084-3
DOI: <http://dx.doi.org/10.1016/j.dsr2.2015.03.007>
Reference: DSR113841

To appear in: *Deep-Sea Research II*

Cite this article as: Jan-Rainer Riethdorf, Benoit Thibodeau, Minoru Ikehara, Dirk Nürnberg, Lars Max, Ralf Tiedemann, Yusuke Yokoyama, Surface nitrate utilization in the Bering sea since 180 kA BP: Insight from sedimentary nitrogen isotopes, *Deep-Sea Research II*, <http://dx.doi.org/10.1016/j.dsr2.2015.03.007>

This is a PDF file of an unedited manuscript that has been accepted for publication. As a service to our customers we are providing this early version of the manuscript. The manuscript will undergo copyediting, typesetting, and review of the resulting galley proof before it is published in its final citable form. Please note that during the production process errors may be discovered which could affect the content, and all legal disclaimers that apply to the journal pertain.

1 **Surface nitrate utilization in the Bering Sea since 180 ka BP: Insight**
2 **from sedimentary nitrogen isotopes**

3
4 **Jan-Rainer Riethdorf^{a,b}, Benoit Thibodeau^{b,c}, Minoru Ikehara^d, Dirk Nürnberg^b,**
5 **Lars Max^e, Ralf Tiedemann^e, and Yusuke Yokoyama^{a,f}**

6
7 ^aDepartment of Ocean Floor Geoscience, Atmosphere and Ocean Research
8 Institute, The University of Tokyo, 5-1-5 Kashiwanoha, Kashiwa, Chiba 277-8564,
9 Japan; jan.riethdorf@gmail.com; yokoyama@aori.u-tokyo.ac.jp

10 ^bHelmholtz Centre for Ocean Research Kiel (GEOMAR), Wischhofstr. 1-3, D-24148
11 Kiel, Germany; dnuernberg@geomar.de; bthibodeau@geomar.de

12 ^cDepartment of Chemical Oceanography, Atmosphere and Ocean Research Institute,
13 The University of Tokyo, 5-1-5 Kashiwanoha, Kashiwa, Chiba 277-8564, Japan

14 ^dCenter for Advanced Marine Core Research, Kochi University, B200 Monobe
15 Nankoku, Kochi 783-8502, Japan; ikehara@kochi-u.ac.jp

16 ^eAlfred Wegener Institute for Polar and Marine Research, Am Handelshafen 12, D-
17 27570 Bremerhaven, Germany; Lars.Max@awi.de; Ralf.Tiedemann@awi.de

18 ^fInstitute of Biogeoscience, Japan Agency for Marine-Earth Science and Technology,
19 Yokosuka 237-0061, Japan

20 **Corresponding author and present adress:**

21 Yusuke Yokoyama

22 Department of Ocean Floor Geoscience

23 Atmosphere and Ocean Research Institute

24 The University of Tokyo

25 5-1-5 Kashiwanoha, Kashiwa Chiba 277-8564, Japan

26 Mail: yokoyama@aori.u-tokyo.ac.jp

27 Phone: +81-4-7136-6141

28

29 Abstract

30 We present high-resolution records of sedimentary nitrogen ($\delta^{15}\text{N}_{\text{bulk}}$) and carbon
31 isotope ratios ($\delta^{13}\text{C}_{\text{bulk}}$) from piston core SO201-2-85KL located in the western Bering
32 Sea. The records reflect changes in surface nitrate utilization and terrestrial organic
33 matter contribution in submillennial resolution that span the last 180 kyr. The $\delta^{15}\text{N}_{\text{bulk}}$
34 record is characterized by a minimum during the penultimate interglacial indicating
35 low nitrate utilization (~62-80%) despite the relatively high export production inferred
36 from opal concentrations along with a significant reduction in the terrestrial organic
37 matter fraction (m_{terr}). This suggests that the consumption of the nitrate pool at our
38 site was incomplete and even more reduced than today (~84%). $\delta^{15}\text{N}_{\text{bulk}}$ increases
39 from Marine Isotope Stage (MIS) 5.4 and culminates during the Last Glacial
40 Maximum, which indicates that nitrate utilization in the Bering Sea was raised during
41 cold intervals (MIS 5.4, 5.2, 4) and almost complete during MIS 3 and 2 (~93-100%).
42 This is in agreement with previous hypotheses suggesting that stronger glacial
43 stratification reduced the nutrient supply from the subeuphotic zone, thereby
44 increasing the iron-to-nutrient ratio and therefore the nitrate utilization in the mixed
45 surface layer. Large variations in $\delta^{15}\text{N}_{\text{bulk}}$ were also recorded from 180 to 130 ka BP
46 (MIS 6), indicating a potential link to insolation and sea-level forcing and its related
47 feedbacks. Millennial-scale oscillations were observed in $\delta^{15}\text{N}_{\text{bulk}}$ and $\delta^{13}\text{C}_{\text{bulk}}$ that
48 might be related to Greenland interstadials.

49

50 **Keywords:** Bering Sea; Quaternary; Nitrogen isotopes; Nitrate utilization

51

52 1. Introduction

53 The polar oceans are thought to have been more stratified during past glacial periods
54 and the breakdown of stratification in the Southern Ocean during interglacials has
55 been suggested as a potential control mechanism for the glacial-interglacial cycles in
56 atmospheric carbon dioxide (CO_2) (for a review see Sigman et al., 2010). Recent
57 studies have found supporting evidence that past variations in stratification/ventilation
58 also occurred in the subarctic North Pacific with implications for ocean-atmosphere

59 gas exchange (Jaccard et al., 2005, 2010; Brunelle et al., 2007, 2010; Galbraith et
60 al., 2008a; Okazaki et al., 2010, 2012; Chikamoto et al., 2012; Menviel et al., 2012;
61 Rella et al., 2012; Jaccard and Galbraith, 2013; Max et al., 2014).

62 The modern subarctic North Pacific is characterized by a permanent halocline due to
63 a low-salinity surface layer that limits the exchange of nutrients between the surface
64 and subsurface and prevents the formation of deep water masses (e.g., Warren,
65 1983; Haug et al., 1999; Emile-Geay et al., 2003). At the same time high marine
66 productivity makes this area a net sink for atmospheric CO₂ (Honda et al., 2002;
67 Takahashi et al., 2002b). However, the efficiency of the biological pump in the high-
68 nutrient, low-chlorophyll (HNLC) regions of the subarctic North Pacific is reduced due
69 to iron limitation (e.g., Tsuda et al., 2003), which results in incomplete nitrate
70 utilization.

71 Sedimentary records from the North Pacific and its marginal seas consistently show
72 reduced contents of biogenic opal and barium, CaCO₃, and organic carbon during
73 past glacial periods, indicating reduced biological export production (e.g.,
74 Gorbarenko et al., 2002; Narita et al., 2002; Kienast et al., 2004; Nürnberg and
75 Tiedemann, 2004; Jaccard et al., 2005, 2010; Okazaki et al., 2005a; Shigemitsu et
76 al., 2007, 2008; Riethdorf et al., 2013a). Restricted marine productivity both in the
77 North Pacific and in the Antarctic sector of the Southern Ocean is attributed to (i) light
78 limitation due to extensive sea-ice coverage (Elderfield and Rickaby, 2000), or (ii) to
79 enhanced stratification of the upper water column that suppressed nutrient supply to
80 the euphotic zone (Francois et al., 1997).

81 Studies investigating these hypotheses applied stable nitrogen isotope ratios ($\delta^{15}\text{N}$)
82 to provide a link to the marine nutrient cycle, but they have been mostly focused on
83 regions not influenced by seasonal sea-ice, which has the potential to modulate
84 biological and terrigenous fluxes. In the NW Pacific the $\delta^{15}\text{N}$ signal can be used as a
85 proxy of surface nitrate utilization, whereas in the NE Pacific, it reflects variations in
86 the composition of the subsurface nitrate pool (Brunelle et al., 2007; Galbraith et al.,
87 2008a). The available reconstructions of surface nitrate utilization in the Okhotsk and
88 Bering seas indicate that in both marginal seas enhanced stratification during glacial
89 intervals resulted in a reduced supply of nitrate to the surface and a more complete

90 utilization of surface nitrate because of the continued iron supply from atmospheric
91 deposition (i.e., higher iron-to-nitrate ratio), thereby explaining the low glacial
92 productivity (e.g., Brunelle et al., 2007, 2010; Kim et al., 2011; Khim et al., 2012).

93 For the Bering Sea, recent studies have found indications for millennial-scale
94 oscillations in export production and terrigenous matter supply, which might be
95 connected to changes in stratification and/or sea-ice influence (Gorbarenko et al.,
96 2005, 2010b; Kim et al., 2011; Riethdorf et al., 2013a; Schlung et al., 2013).
97 However, most of the available records of $\delta^{15}\text{N}$ are located in the southern Bering
98 Sea and therefore not necessarily influenced by seasonal sea-ice. Moreover, the
99 records are restricted to ~120 ka BP and do not allow for a comparison between the
100 glacial terminations, which due to the large amplitude of climate and environmental
101 changes are considered important periods for the understanding of the carbon cycle
102 (e.g., Yokoyama and Esat, 2011). Especially for Marine Isotope Stage 6 (MIS 6),
103 which in the Okhotsk Sea environment is characterized by rather extreme glacial ice
104 conditions with significantly increased accumulation rates of ice-rafted debris (IRD)
105 (Nürnberg et al., 2011), no records of $\delta^{15}\text{N}$ are available.

106 Here, we present isotope geochemical records from a supposedly sea-ice influenced
107 site in the poorly studied western Bering Sea for the last 180 kyr in high-resolution
108 employing sedimentary carbon and nitrogen isotope ratios to reconstruct changes in
109 the contribution of terrestrial organic matter and surface nitrate utilization,
110 respectively. Our results, for the first time, provide information on nitrate utilization in
111 the Bering Sea beyond 120 ka BP and expand the hypothesis of glacial-interglacial
112 stratification changes to cold and warm intervals. Moreover, our record suggests that
113 millennial-scale climate oscillations occurred in the Bering Sea which might be
114 connected to Greenland interstadials.

115

116 **2. Study area**

117 The Bering and Okhotsk seas are marginal seas of the North Pacific, separated from
118 by the Aleutian and Kurile islands, respectively. They are bounded by the coasts of
119 eastern Siberia, the Kamchatka Peninsula and/or western Alaska. Wide and shallow

120 continental shelf areas are found in the northern Okhotsk and in the northern and
121 eastern Bering Sea (Figure 1).

122 With respect to surface circulation, waters from the North Pacific are transported
123 westward along the Aleutian islands by the Alaskan Stream and enter the Bering Sea
124 via the Aleutian passes. There, the Bering Slope Current (BSC) and the East
125 Kamchatka Current (EKC) form boundary currents (Stabeno et al., 1999). Surface
126 outflow is directed into the Arctic Ocean through the shallow (~50 m) Bering Strait,
127 whereas surface and deeper waters are transported back into the NW Pacific through
128 the deeper straits, mainly Kamchatka Strait (Figure 1). The EKC and the Oyashio
129 current flow southward and represent western boundary currents of the North Pacific
130 subpolar gyre. The Kurile straits provide entrance and exit pathways to the Okhotsk
131 Sea.

132 Major climatic and oceanographic characteristics of the North Pacific realm are the
133 strong seasonality in sea surface temperatures (SST) and sea-ice formation, the
134 permanent halocline, and a pronounced oxygen minimum zone (OMZ). In the Bering
135 Sea sea-ice is present from September until July reaching its maximum distribution
136 during March/April (Tomczak and Godfrey, 1994; Niebauer et al., 1999). The sea-ice
137 formation is related to the interaction of the Siberian High and the Aleutian Low,
138 which results in the advection of cold Arctic air masses, subsequent cooling of the
139 sea surface, and strong winter mixing (Stabeno et al., 1999). Sea-ice is considered
140 as an important transport agent of terrigenous matter in the Okhotsk and Bering seas
141 (Nürnberg and Tiedemann, 2004; Nürnberg et al., 2011; Riethdorf et al., 2013a).
142 Geochemical results indicate that sediments on the eastern Bering Sea shelf and in
143 the Meiji Drift in the NW Pacific are supplied from Yukon–Bering Sea sources
144 (VanLaningham et al., 2009; Asahara et al., 2012; Nagashima et al., 2012). Based on
145 these results Riethdorf et al. (2013a) proposed that terrigenous matter entrained into
146 sea-ice by tidal pumping, suspension freezing, and beach-ice formation, was
147 transported from the eastern Bering Sea shelf to the location studied in this paper,
148 although a contribution by suspension load carried by the BSC could not be
149 excluded.

150 Although sea-ice formation and according brine rejection in the northern Okhotsk Sea
151 drive the modern ventilation of North Pacific Intermediate Water (NPIW) (e.g.,
152 Yasuda, 1997; Yamamoto et al., 2001), the source of NPIW might have shifted to the
153 Bering Sea in the past (Matsumoto et al., 2002; Ohkushi et al., 2003; Tanaka and
154 Takahashi, 2005; Rella et al., 2012), where it nowadays resides at the depth of the
155 26.8 potential density (σ_θ) surface in ~200-400 m (Roden, 1995; Macdonald et al.,
156 2001). The OMZ is found beneath the NPIW with minimum dissolved oxygen
157 concentrations of ~15-20 $\mu\text{mol kg}^{-1}$ at ~900-1100 m (Roden, 2000; Lehmann et al.,
158 2005).

159 In the Bering Sea, high marine productivity is observed, which is mainly associated
160 with shelf areas (e.g., Springer et al., 1996; Stabeno et al., 1999) and dominated by
161 diatoms. Major biological fluxes occur during spring/summer (mainly diatoms) and
162 late summer/early fall (coccolithophores and planktonic foraminifera) (Takahashi et
163 al., 2002a). Nutrients are consumed during the productive seasons and returned from
164 the subsurface by winter mixing. Although winter mixing supplies nutrients from the
165 subsurface into the euphotic zone, near-surface nutrients are not completely
166 consumed by phytoplankton during the productive seasons. Therefore, the western
167 Bering Sea studied here, as well as the central eastern and western parts of the
168 subarctic North Pacific are HNLC regions with perennially high surface nitrate
169 concentrations (e.g., Tyrrell et al., 2005) (Figure 1). As extensively discussed in
170 Brunelle et al. (2007, 2010) changes in the extent of surface nitrate utilization can be
171 reconstructed using records of $\delta^{15}\text{N}$, if the underlying assumptions include a constant
172 isotope effect for nitrate assimilation and little or no changes in the $\delta^{15}\text{N}$ of the source
173 nitrate. There is evidence for the northward propagation of ^{15}N -enriched nitrate from
174 the eastern tropical North Pacific along coastal North America (Liu and Kaplan, 1989;
175 Altabet et al., 1999; Kienast et al., 2002; Sigman et al., 2003). Hence,
176 paleoceanographic interpretations of sedimentary $\delta^{15}\text{N}$ have to consider changes in
177 the $\delta^{15}\text{N}$ of the subsurface nitrate pool.

178

179

180

181 3. Material and methods

182 This study is based on 18.13 m-long piston core SO201-2-85KL (referred to as 85KL
183 hereafter) recovered during R/V Sonne expedition SO201 KALMAR Leg 2 in 2009
184 (Dullo et al., 2009) from Shirshov Ridge, western Bering Sea (57°30.30'N,
185 170°24.77'E, 968 m water depth; Figure 1). Sediments from this core mainly consist
186 of terrigenous siliciclastic material bound to the clay- and silt-fractions, but layers of
187 diatomaceous ooze are repeatedly intercalated. Carbonate preservation is poor and
188 at best sporadic, and no sediments younger than 7.5 ka BP were recovered.

189

190 3.1 Bulk sedimentary analyses (TOC, TN, $\delta^{13}\text{C}_{\text{bulk}}$, $\delta^{15}\text{N}_{\text{bulk}}$)

191 Total organic carbon (TOC) and total nitrogen (TN) concentrations, as well as
192 sedimentary stable carbon ($\delta^{13}\text{C}_{\text{bulk}}$) and nitrogen ($\delta^{15}\text{N}_{\text{bulk}}$) isotope ratios were
193 determined downcore (>9.1 ka BP) every 5 cm from a total of 357 bulk sediment
194 samples. About 25 mg of freeze-dried, hand-ground (agate mortar) sediment was
195 weighed into Ag capsules, acidified with 100 μl hydrochloric acid (3N) to remove
196 inorganic carbon, and dried in a desiccator filled with phosphorus pentoxide and
197 sodium hydroxide. To ensure complete combustion, the Ag capsules were
198 subsequently wrapped into Sn capsules. TOC, TN, $\delta^{13}\text{C}_{\text{bulk}}$, and $\delta^{15}\text{N}_{\text{bulk}}$ were
199 determined at the Center for Advanced Marine Core Research, Kochi University,
200 using a Flash EA 1112 Series elemental analyzer (EA; Thermo Fisher Scientific,
201 USA) coupled with a Delta Plus Advantage isotope ratio mass spectrometer (IRMS;
202 Thermo Fisher Scientific, USA) via a Conflo III interface (He carrier). Stable isotope
203 results are reported in conventional δ -notation and referenced to the Vienna PeeDee
204 Belemnite (VPDB) standard and to atmospheric nitrogen. Molar TN/TOC ratios were
205 corrected for inorganic nitrogen compounds based on a linear regression between
206 TOC and TN following Goñi et al. (1998) (referred to as molar N/C ratios hereafter;
207 Figure 2). Analytical precision (1σ) was determined from two different standards (L-
208 Alanine, $n = 58$; Sulfanilamide, $n = 60$) and was <2% RSD (relative standard
209 deviation) for TOC, <5% RSD for TN, ± 0.01 for molar N/C ratio, $\pm 0.14\text{‰}$ for $\delta^{13}\text{C}_{\text{bulk}}$,
210 and $\pm 0.29\text{‰}$ for $\delta^{15}\text{N}_{\text{bulk}}$. Reproducibility of the samples, determined from replicates
211 (1σ , $n = 14$), was ± 0.01 wt.% for TOC and TN, ± 0.01 for molar N/C ratio, $\pm 0.11\text{‰}$ for

212 $\delta^{13}\text{C}_{\text{bulk}}$, and $\pm 0.86\text{‰}$ for $\delta^{15}\text{N}_{\text{bulk}}$. This rather high value for $\delta^{15}\text{N}_{\text{bulk}}$, being significantly
213 higher than instrumental precision, might be related to sample inhomogeneity and
214 potential alteration of the sedimentary organic matter during pre-analysis acid
215 treatment (Brodie et al., 2011a, 2011b).

216

217 **3.2 Age model**

218 The stratigraphic framework of 85KL is described in detail in Max et al. (2012) and
219 Riethdorf et al. (2013a). Briefly, X-ray fluorescence (XRF) and spectrophotometric
220 (color b^*) core logging data were correlated to the $\delta^{18}\text{O}$ records of the NGRIP ice
221 core (NGRIP members, 2004; GICC05 timescale, Rasmussen et al., 2006) and the
222 Sanbao stalagmites (Wang et al., 2008). This approach was validated by benthic
223 $\delta^{18}\text{O}$ stratigraphy, magnetostratigraphy, accelerator mass spectrometry (AMS)
224 radiocarbon dating of planktonic foraminifera, and intercore correlations to
225 neighbouring sediment cores. Linear sedimentation rates vary between 4 and 23 cm
226 kyr^{-1} (average of $\sim 12 \text{ cm kyr}^{-1}$), which translates into a submillennial time-resolution
227 for our reconstructions.

228

229 **3.3 Existing data**

230 For comparison we used logging data and geochemical results reflecting changes in
231 export production and terrigenous matter supply already available for core 85KL.
232 Method details are given elsewhere (Max et al., 2012; Riethdorf et al., 2013a,
233 2013b). In summary, light and color reflectance were measured directly after core
234 recovery every 1 cm using a Minolta CM 508d hand-held spectrophotometer and
235 converted into *Commission Internationale de l'Éclairage* (CIE) L^* , a^* , and b^* color
236 space. XRF scanning for elements Al through to Ba was performed at 1 cm sampling
237 resolution using the Avaatech XRF core scanner at Alfred Wegener Institute for Polar
238 and Marine Research, Bremerhaven. Molybdate-blue spectrophotometry was used to
239 determine biogenic opal concentrations (after Müller and Schneider, 1993), and
240 concentrations of CaCO_3 were calculated from the difference of total carbon (TC) and
241 TOC previously determined using a Carlo Erba CNS analyzer (model NA-1500) at

242 GEOMAR, Kiel. The relative amount of siliciclastics was calculated by subtracting the
243 sum of CaCO_3 , TOC, and opal concentrations from a total of 100 wt.%. Records of
244 XRF Ca/Ti log-ratios, XRF Br count rates (in counts per second, cps), and color b^*
245 correlated with CaCO_3 ($R^2 = 0.65$), TOC ($R^2 = 0.64$), and opal ($R^2 = 0.61$),
246 respectively. This finding is in agreement with other studies linking biogenic CaCO_3
247 with normalized XRF records of Ca (Jaccard et al., 2005), TOC with biophilic Br
248 (Ziegler et al., 2008), and opal and organic matter content with color b^* (Debret et al.,
249 2006).

250

251 **3.4 Reconstruction of export production**

252 The use of CaCO_3 , TOC, and opal to reconstruct changes in export production is
253 subject to specific restrictions. CaCO_3 , especially in the North Pacific, is influenced
254 by carbonate dissolution and might be more indicative of changes in the bottom
255 water calcite saturation state (e.g. Jaccard et al., 2005). With respect to TOC, it is
256 necessary to discriminate between marine and terrestrial carbon sources. The most
257 often used proxy for reconstructions of paleo-export production in the North Pacific
258 realm is biogenic opal (e.g. Kienast et al., 2004).

259 In paleoceanography, fluxes are usually reconstructed using accumulation rates
260 rather than proxy concentrations. However, for the North Pacific and Bering Sea
261 several studies provide evidence for the similar evolution of concentration and
262 accumulation records of biogenic components (e.g. Crusius et al., 2004; Brunelle et
263 al., 2007, 2010). Here, we used dry bulk density measurements (Riethdorf et al.,
264 2013a) to calculate bulk mass accumulation rates (AR Bulk, in $\text{g cm}^{-2} \text{ kyr}^{-1}$), as well
265 as proxy accumulation rates for CaCO_3 , TOC, opal, and siliciclastics. The result is
266 shown in Figure 3, clearly demonstrating that sedimentation at Site 85KL is
267 dominated by siliciclastic input. Overall, concentrations of the biogenic components
268 are low, but opal concentrations and opal accumulation rates show a positive linear
269 relationship ($R^2 = 0.49$). We therefore assume in this paper that at Site 85KL
270 concentrations of opal and color b^* logging data are related to export production.

271

272

273 4. Results

274 4.1 Export production and terrigenous matter supply

275 In general, concentrations of CaCO_3 , TOC, and opal, as well as their approximating
276 logging data show increased values during warm intervals (MIS 5.5, 5.3, 5.1, and 1)
277 and Greenland interstadials (GI), but low values during cold intervals (MIS 6, 5.4, 5.2,
278 4, and 2) and Greenland stadials (GS) (Figure 4; Riethdorf et al., 2013a). Because of
279 sedimentary dilution, the proxy records reflecting terrigenous matter supply
280 (%Siliciclastics, XRF data of Al) have an inversed shape with respect to the records
281 reflecting export production. Our EA-IRMS-based TOC results are in excellent
282 agreement with those of Riethdorf et al. (2013a) and in higher temporal resolution
283 extend the respective record by ~ 30 kyr into MIS 6. The temporal evolution of TOC
284 recorded during MIS 6 strongly corresponds to that observed in color b^* , and, to a
285 lesser degree, in XRF Ca/Ti log-ratios and Br count rates (Figure 4). With respect to
286 TOC concentrations, MIS 6 is characterized by a strong variability within the range of
287 ~ 0.4 to ~ 1.7 wt.%, showing several short-lived oscillations and highest
288 concentrations during ~ 156 -137 ka BP.

289

290 4.2 $\delta^{13}\text{C}_{\text{bulk}}$, $\delta^{15}\text{N}_{\text{bulk}}$, molar N/C ratios, and estimation of the terrestrial organic 291 matter fraction (m_{terr})

292 Values for $\delta^{13}\text{C}_{\text{bulk}}$ (of TOC) and for $\delta^{15}\text{N}_{\text{bulk}}$ (of TN) ranged from -25.4 to -21.9‰ and
293 from 1.7 to 7.5‰ , respectively, and molar N/C ratios varied between 0.04 and 0.11
294 (Table 1; Figures 5 and 6). In general, $\delta^{13}\text{C}_{\text{bulk}}$ and molar N/C ratios are more positive
295 during warm intervals (MIS 5.5, 5.3, 5.1, 3, and 1) and show pronounced, but short-
296 lived maxima during GI, which especially for $\delta^{13}\text{C}_{\text{bulk}}$ exceed analytical precision and
297 reproducibility. The cold intervals (MIS 5.4, 5.2, and 4) and some GS are
298 characterized by decreases in both proxies. A different temporal evolution is
299 recorded for $\delta^{15}\text{N}_{\text{bulk}}$. The base of core 85KL shows $\delta^{15}\text{N}_{\text{bulk}}$ values of ~ 5 - 6‰ , which
300 is followed by a sharp decrease at ~ 172 ka BP to values of ~ 2 - 3‰ (Figure 6).
301 Subsequently, $\delta^{15}\text{N}_{\text{bulk}}$ again increases until another sudden drop of $\sim 3\text{‰}$
302 characterizes the transition from MIS 6 to 5.5 (Termination II). During the last

303 interglacial $\delta^{15}\text{N}_{\text{bulk}}$ remained low at $\sim 3\text{‰}$ but it decreased even further to minimum
304 values of 1.7‰ at the beginning of cold MIS 5.4. After MIS 5.4, a long-term trend
305 toward higher values that continues into the early Holocene is observed. In between,
306 increasing values were recorded during cold MIS 5.2 and 4, whereas $\delta^{15}\text{N}_{\text{bulk}}$
307 decreased (MIS 5.1) or remained almost constant (MIS 5.3 and 3) during warm
308 stages. The transition from MIS 2 to 1 (Termination I) is characterized by local
309 minima ($\sim 4\text{-}5\text{‰}$) during the cold phases of Heinrich Stadial 1 (HS1; 18.0-14.7 ka BP,
310 Sarnthein et al., 2001) and the Younger Dryas (YD; 12.9-11.7 ka BP, Blockley et al.,
311 2012), and by an intercalated pronounced maximum during the Bølling-Allerød warm
312 phase (B/A; 14.7-12.9 ka BP, Blockley et al., 2012) (up to 6.8‰). Subsequent to the
313 YD, $\delta^{15}\text{N}_{\text{bulk}}$ continuously increased until highest values of 7.5‰ were recorded
314 during the early Holocene (~ 10.1 ka BP). Notably, the $\delta^{15}\text{N}_{\text{bulk}}$ record also features
315 short-lived maxima during GI, which, however, must be considered insignificant with
316 respect to reproducibility.

317 Assuming that the geochemical and isotopic sedimentary composition represents a
318 mixture of marine and terrestrial organic matter we applied a linear mixing model to
319 estimate the fraction of terrestrial-derived organic matter (m_{terr}) using hypothetical
320 endmember compositions. We therefore followed the results of Walinsky et al.
321 (2009). This approach has recently been applied to a sediment core from the
322 northern Gulf of Alaska (Addison et al., 2012). Our Holocene samples lie within the
323 ranges reported by Smith et al. (2002) for surface sediment samples from the
324 southeastern Bering Sea shelf, whereas our glacial samples compare to terrigenous
325 particulate organic matter (POM) from the Yukon River (Guo and Macdonald, 2006)
326 (Figure 5). Accordingly, we assume that the most likely organic matter sources for
327 our site are marine phytoplankton ($\delta^{13}\text{C}$: -22 to -20‰ ; $\delta^{15}\text{N}$: $>5\text{‰}$; molar N/C ratio:
328 0.10 to 0.15), soil ($\delta^{13}\text{C}$: -26.5 to -25.5‰ ; $\delta^{15}\text{N}$: 0 to 1‰ ; molar N/C ratio: 0.08 to
329 0.10), and vascular plant detritus (VPD; $\delta^{13}\text{C}$: -27 to -25‰ ; $\delta^{15}\text{N}$: 0 to 1‰ ; molar N/C
330 ratio: 0 to 0.05) (Meyers, 1994; McQuoid et al., 2001; Geider and La Roche, 2002;
331 Smith et al., 2002; Guo et al., 2004; Gaye-Haake et al., 2005; Guo and Macdonald,
332 2006; Walsh et al., 2008, and references therein) (Figure 5; Table 2). With the
333 influence of soil considered insignificant, m_{terr} was calculated as:

$$m_{\text{terr}} = (A_{\text{sample}} - A_{\text{mar}}) / (A_{\text{terr}} - A_{\text{mar}}) \quad (\text{Eq. 1})$$

334
 335 In Equation 1 A refers to the $\delta^{13}\text{C}_{\text{bulk}}$ or molar N/C ratio of the sample and the
 336 respective average values for the assumed marine and terrestrial endmember
 337 composition summarized in Table 2. We preferred using molar N/C over C/N ratios,
 338 because mixing lines based on C/N are reported to underestimate the fraction of
 339 terrestrially derived organic carbon (Perdue and Koprivnjak, 2007). This approach
 340 resulted in similar values but in part different temporal evolutions of the respective
 341 m_{terr} records, which is attributed to the low variability in molar N/C ratios. m_{terr} varied
 342 between ~10% and ~90% with average values of ~40-50% (Table 1). It was lowest
 343 during warm intervals (MIS 5.5, 5.3, 5.1, 3, and 1) and GI, when marine productivity
 344 was high. Reductions of up to 50% occurred during the transitions from cold to warm
 345 intervals, whereas pronounced but short-lived increases of ~20% seem to
 346 correspond to GS (Figure 6). In the discussion we refer to m_{terr} derived from $\delta^{13}\text{C}_{\text{bulk}}$.

347

348 5. Discussion

349 5.1 The $\delta^{15}\text{N}_{\text{bulk}}$ signal and potential alteration

350 $\delta^{15}\text{N}_{\text{bulk}}$ values reflect the isotopic signature of the export flux of organic matter plus
 351 any secondary alteration of this signal during sinking and burial (e.g., Galbraith et al.,
 352 2008b; Robinson et al., 2012, and references therein). Hence, interpretation of
 353 variations in the $\delta^{15}\text{N}_{\text{bulk}}$ record must consider changes in (i) the isotopic composition
 354 of the subsurface nitrate pool, which is controlled by nitrogen fixation by diazotrophic
 355 bacteria and by denitrification, (ii) the degree of nitrification and surface nitrate
 356 utilization, and (iii) secondary alteration.

357 Nitrate is the primary nitrogen source for marine phytoplankton, which preferentially
 358 incorporates isotopically light (^{14}N -enriched) nitrate (Pennock et al., 1996; Waser et
 359 al., 1998). In the Bering Sea the source nitrate is supplied to the surface from below
 360 the euphotic zone with a modern value ($\delta^{15}\text{N}_{\text{nitrate}}$) of ~5.5‰ (Lehmann et al., 2005),
 361 which is slightly higher than the global deep ocean average of ~5‰ because of
 362 denitrification in the North Pacific (Sigman et al., 2000, Brunelle et al., 2007).
 363 Nitrogen fixation results in $\delta^{15}\text{N}_{\text{nitrate}}$ values that are isotopically light and close to that

364 of air (0‰; Carpenter et al., 1997), and it is the main reason for the low $\delta^{15}\text{N}$ values
365 of nitrate and sinking detritus in the tropical/subtropical ocean basins (e.g., Some et
366 al., 2010). Water column denitrification occurs under low dissolved oxygen
367 concentrations ($<5 \mu\text{mol l}^{-1}$; Codispoti et al., 2001) and results in a ^{15}N -enriched
368 nitrate pool (Barford et al., 1999). In this respect, $\delta^{15}\text{N}$ might also reflect redox
369 conditions in the past with higher values during bottom water suboxia (Galbraith et
370 al., 2004; Kashiyama et al., 2008; Jaccard and Galbraith, 2012; Robinson et al.,
371 2012). Today, water column denitrification is mainly observed in the Arabian Sea, the
372 eastern tropical North Pacific, and in the eastern tropical South Pacific. Thus, the
373 export of ^{15}N -enriched waters might result in a shift toward higher $\delta^{15}\text{N}_{\text{nitrate}}$, as
374 observed along coastal North America in the subarctic NE Pacific (Liu and Kaplan,
375 1989; Altabet et al., 1999; Kienast et al., 2002; Sigman et al., 2003). However,
376 modern dissolved oxygen concentrations at Site 85KL lie above the denitrification
377 threshold.

378 Results from benthic foraminiferal assemblages from the same site (Ovsepyan et al.,
379 2013) suggest oxidizing conditions in the surface sediment layer from MIS 3 to the
380 Last Glacial Maximum (LGM), but oxygen-depleted conditions during the mid-B/A
381 and early Holocene. This is in agreement with Kim et al. (2011) who for Site PC23A
382 reported on a dominance of oxic benthic foraminiferal species during MIS 2 and 3,
383 but on dominantly dysoxic species during the B/A, early Holocene, and GI. These
384 observations and our proxy records for export production indicate the presence of
385 mostly oxic bottom waters and strongly reduced export of organic matter during most
386 of the past 180 kyr, arguing against a significant impact of water column
387 denitrification on $\delta^{15}\text{N}_{\text{bulk}}$. Over the last 180 kyr, one can expect a slightly higher $\delta^{15}\text{N}$
388 of nitrate during warm stages because of the greater extent of denitrification in the
389 North Pacific. The isotopic impact of such increased denitrification during warm
390 stages is thought to be relatively equal to the one observed today ($\sim 0.5\%$; Lehmann
391 et al., 2005). This shift toward heavier $\delta^{15}\text{N}$ is opposite to the expected isotopic effect
392 of decreased nitrate utilization during interglacials. Thus, the relatively small increase
393 in $\delta^{15}\text{N}_{\text{bulk}}$ during warm stages ($\sim 0.5\%$) should not mask the larger isotopic variation
394 expected from the change in nitrate utilization (Brunelle et al., 2007, and references
395 therein). Thus, we are confident that the observed variations in our $\delta^{15}\text{N}_{\text{bulk}}$ can be

396 used to assess relative changes in the utilization of nitrate in the Bering Sea surface
 397 water, except for periods where dysoxia were locally present. During phases of
 398 locally enhanced export production and oxygen-depleted bottom water conditions, as
 399 recorded during the B/A and the early Holocene, as well as during GI, denitrification
 400 might have resulted in a shift toward heavier $\delta^{15}\text{N}_{\text{bulk}}$ values. Because we can not
 401 isolate this signal in our record, our nitrate utilization estimates for these periods
 402 might not be accurate due to potential changes in the $\delta^{15}\text{N}$ signature of the source
 403 nitrate

404 Nitrate utilization is incomplete in the modern subarctic North Pacific and in the
 405 Bering Sea. Accordingly, the isotopic value of the export flux of organic matter
 406 ($\delta^{15}\text{N}_{\text{export}}$) is lighter than that of $\delta^{15}\text{N}_{\text{nitrate}}$ (Altabet and Francois, 1994; Sigman et al.,
 407 1999; Needoba et al., 2003; Galbraith et al., 2008a). The difference between
 408 $\delta^{15}\text{N}_{\text{nitrate}}$ and $\delta^{15}\text{N}_{\text{export}}$ is primarily controlled by the nitrate utilization and decreases
 409 as it becomes more complete and in most of the global ocean the difference is zero
 410 due to almost complete utilization (Altabet et al., 1999; Thunell et al., 2004). We can
 411 calculate $\delta^{15}\text{N}_{\text{export}}$ for the expected integrated organic nitrogen export at Site 85KL
 412 assuming Rayleigh fractionation kinetics (Altabet and Francois, 1994; Mariotti et al.,
 413 1981) after:

$$414 \quad \delta^{15}\text{N}_{\text{export}} = \delta^{15}\text{N}_{\text{nitrate}} + f / (1 - f) \varepsilon \ln (f) \quad (\text{Eq. 2})$$

415 In Equation 2 f is the fraction of unutilized nitrate (i.e., $[\text{NO}_3^-]_{\text{summer}} / [\text{NO}_3^-]_{\text{winter}}$) and ε
 416 is the isotope effect for nitrate incorporation by phytoplankton, which was assumed to
 417 be constant at $\sim 5\text{‰}$ for simplification (Brunelle et al., 2007, 2010). Using a modern
 418 average for f of 0.16 (84% utilization), estimated from WOA 2009 surface nitrate
 419 concentrations (Garcia et al., 2010), gives $\delta^{15}\text{N}_{\text{export}} = \sim 3.8\text{‰}$ for our site, which is
 420 1.7‰ lower than the modern $\delta^{15}\text{N}_{\text{nitrate}}$. Unfortunately, no coretop $\delta^{15}\text{N}_{\text{bulk}}$ results are
 421 available for verification at our site.

422 Alternatively, secondary alteration (preferential loss of organic nitrogen, leakage of
 423 ammonium into pore waters, ammonium absorption into clay minerals,
 424 winnowing/size fractionation) might have raised the modern coretop $\delta^{15}\text{N}$ value. In
 425 general, however, alteration of the $\delta^{15}\text{N}_{\text{bulk}}$ from that of the sinking flux is not

426 considered to have a considerable influence in organic-rich sediments from high-
427 accumulation regions with low contributions of inorganic nitrogen compounds (for a
428 review see Robinson et al., 2012). Core 85KL has rather high average TOC
429 concentrations (~0.9 wt.%), whereas TIN is low at ~0.017 wt.% (Figure 2a), and the
430 relationship between TN and $\delta^{15}\text{N}_{\text{bulk}}$ is only weak ($R^2 = 0.24$; Figure 2b), which
431 argues against alteration. Moreover, in comparison with other Bering Sea records
432 using $\delta^{15}\text{N}$ as a proxy for nitrate utilization (Brunelle et al., 2007, 2010; Kim et al.,
433 2011; Schlung et al., 2013) our $\delta^{15}\text{N}_{\text{bulk}}$ record generally shows a similar evolution
434 (Figure 7). Notably, at our study site $\delta^{15}\text{N}_{\text{bulk}}$ values $>5.5\text{‰}$ were mainly recorded
435 during Termination I, which, in accordance with the previously mentioned studies is
436 more likely attributed to enhanced deglacial water column denitrification.

437 Finally, there might have been influence from terrestrial nitrogen, since our estimates
438 for m_{terr} suggest significant average contributions (~40-50%) of terrestrial organic
439 matter in Shirshov Ridge sediments. In this respect, variations in $\delta^{15}\text{N}_{\text{bulk}}$ might reflect
440 changes in the supply of terrestrial nitrogen. However, for the estimation of m_{terr} we
441 assumed that the $\delta^{15}\text{N}_{\text{bulk}}$ of terrestrial organic matter is lower than that of marine
442 organic matter. If there was considerable influence from terrestrial nitrogen we would
443 expect a strong positive relationship between molar N/C ratios and $\delta^{15}\text{N}_{\text{bulk}}$, which is
444 not observed ($R^2 = 0.10$). Accordingly, although Site 85KL is characterized by overall
445 high m_{terr} values with a strong downcore variability, there seems to have been no
446 significant influence of m_{terr} on the $\delta^{15}\text{N}_{\text{bulk}}$ signal, which might be explained by an
447 only low fraction of terrestrial nitrogen. We therefore consider the influence of
448 secondary alteration and contamination from terrestrial nitrogen on the $\delta^{15}\text{N}_{\text{bulk}}$ signal
449 as insignificant and in the following discuss variations in $\delta^{15}\text{N}_{\text{bulk}}$ by means of
450 changes in surface nitrate utilization.

451

452 **5.2 Cold and warm intervals of the past 180 kyr**

453 At Site 85KL, glacial periods, specifically cold intervals (MIS 6, 5.4, 5.2, and 4 to 2),
454 were characterized by significantly reduced export production and enhanced
455 terrigenous matter supply (Riethdorf et al., 2013a; Figure 4), which is in agreement

456 with other studies from the subarctic North Pacific (e.g., Kienast et al., 2004; Jaccard
457 et al., 2005), the Okhotsk Sea (e.g., Narita et al., 2002; Nürnberg and Tiedemann,
458 2004; Okazaki et al., 2005b; Nürnberg et al., 2011), and the Bering Sea (e.g.,
459 Okazaki et al., 2005a; Brunelle et al., 2007; Kim et al., 2011). This is supported by
460 our reconstruction of m_{terr} indicating an average terrestrial organic matter fraction of
461 ~40-50%, which is significantly reduced only during warm intervals. Today, the
462 organic matter in Bering Sea sediments is dominantly of marine origin (Méheust et
463 al., 2013). The glacial terrigenous matter source of Bering Sea sediments is under
464 debate, but there are indications that they originate from source rocks drained by the
465 Yukon River (VanLaningham et al., 2009), and/or from sea-ice rafting in the NE
466 Bering Sea (Riethdorf et al., 2013a).

467 For the Bering and Okhotsk seas the outlined observations were explained by
468 enhanced sea-ice influence and stronger stratification of the upper water column
469 during cold climate conditions restricting marine productivity (Nürnberg and
470 Tiedemann, 2004; Brunelle et al., 2007, 2010; Kim et al., 2011; Khim et al., 2012;
471 Riethdorf et al., 2013a). This restriction results from the extended sea-ice season and
472 coverage and the subsequent limitation of light availability and vertical mixing
473 (nutrient supply), but temperature limitation is likely to have played an additional role.
474 An extended Bering Sea sea-ice coverage during cold phases is supported by
475 reconstructions from diatom assemblages (Katsuki and Takahashi, 2005) and from
476 the diatom-derived, highly branched isoprenoid sea ice biomarker (IP₂₅) (Max et al.,
477 2012).

478 Records of sedimentary and diatom-bound $\delta^{15}N$ imply enhanced surface nitrate
479 utilization as a result of stronger upper water column stratification in the Bering Sea,
480 especially during MIS 3 and 2 (Brunelle et al., 2007, 2010; Kim et al., 2011). Similar
481 observations are reported for the Okhotsk Sea (Brunelle et al., 2010; Khim et al.,
482 2012) and the subarctic NW Pacific (Galbraith et al., 2008a; Brunelle et al., 2010),
483 indicating that these regions were not always HNLC. This shift towards higher $\delta^{15}N$ in
484 MIS 3 is, however, not observed at IODP Site U1340 at the northeastern flank of
485 Bowers Ridge (Schlung et al., 2013). Instead, a sharp decrease in $\delta^{15}N_{bulk}$ was
486 recorded at this site at ~55 ka BP, which might be related to local stratification
487 changes, or to the influence of turbidites that are reported to compromise records

488 recovered from that area (Nakatsuka et al., 1995). Our $\delta^{15}\text{N}_{\text{bulk}}$ results are in
489 accordance with the former Bering Sea studies confirming enhanced nitrate
490 utilization during cold intervals, but they seem to reveal a more complex development
491 of stratification and for the first time provide information for MIS 6.

492 At the base of core 85KL (~180-173 ka BP), early MIS 6 is characterized by high
493 $\delta^{15}\text{N}_{\text{bulk}}$ values indicating almost complete nitrate utilization, when export production
494 was reduced, but maintained. Relatively high $\delta^{15}\text{N}_{\text{bulk}}$ during MIS 6 were also
495 recorded at Okhotsk Sea sites GGC27 (Brunelle et al., 2010) and GC9A (Khim et al.,
496 2012), as well as at ODP Site 882 and at Site MD01-2416 (Galbraith et al., 2008a).
497 Hence, low insolation and weak seasonal contrasts most probably caused a
498 prolonged sea-ice season, extended sea-ice coverage, and suppressed vertical
499 mixing. At ~172 ka BP, when Northern Hemisphere summer insolation had a local
500 maximum, a sharp decrease in $\delta^{15}\text{N}_{\text{bulk}}$ implies a sudden drop in nitrate utilization
501 (from ~100% to ~50-70%) in the Bering Sea (Figure 6). At the same time export
502 production was increased, whereas m_{terr} decreased. This might be explained by a
503 shortened sea-ice season, reduced sea-ice coverage, and enhanced winter mixing
504 due to stronger seasonal contrasts, which increased the nutrient supply from the
505 subeuphotic zone.

506 Accordingly, we speculate that changes in nitrate utilization are strongly affected by
507 insolation forcing and a feedback by sea-ice processes that drive the extent of
508 vertical mixing during winter, as well as the input of terrestrial organic matter.
509 Dominant climate control via insolation has already been proposed for the Okhotsk
510 Sea (Gorbarenko et al., 2010a, 2012). The long-term increase in nitrate utilization
511 after ~172 ka BP until Termination II, which is also observed at the Okhotsk Sea and
512 NW Pacific sites (Figure 7), as well as the long-term increase from MIS 5.4 until
513 Termination I might be explained by increasingly fostered stratification (i.e. a
514 reduction in the supply of nutrients into the euphotic zone), which is finally subject to
515 a 'breakdown' during the deglaciations. It is beyond the scope of this paper to
516 decipher the underlying causes of this deglacial breakdown, but increasing insolation
517 resulting in a reduced sea-ice season and strengthened winter mixing, is a likely
518 contributing factor.

519 The observation that the strongest maxima in Northern Hemisphere summer
520 insolation, mainly those of warm intervals (MIS 5.5, 5.3, 5.1, and 1), are reflected by
521 maxima in export production (Figure 4), minima in m_{terr} , and decreasing or constant
522 $\delta^{15}\text{N}_{\text{bulk}}$ (Figure 6), supports the view that insolation changes affect nutrient-limited
523 marine productivity by a feedback in sea-ice processes and winter mixing. It is also in
524 agreement with previously published concepts proposed to explain glacial-interglacial
525 changes in the Okhotsk (Seki et al., 2004; Okazaki et al., 2005b; Khim et al., 2012)
526 and Bering seas (Nakatsuka et al., 1995; Kim et al., 2011). When applying Equation
527 2, our $\delta^{15}\text{N}_{\text{bulk}}$ record indicates increasing nitrate utilization during cold MIS 5.4 (from
528 ~50 to ~90%), MIS 5.2 (from ~90 to ~100%), and MIS 4 (from ~80 to ~93%), and
529 almost complete utilization during MIS 3 and 2 (~93-100%). On the other hand,
530 decreasing or constant nitrate utilization was recorded during warm MIS 5.5 (from
531 ~97 to ~62%), MIS 5.3 (~90%), and MIS 5.1 (from ~100 to ~80%). This suggests that
532 stratification was fostered during cold intervals, but weakened during warm intervals
533 due to the processes outlined above.

534 The low glacial $\delta^{15}\text{N}_{\text{bulk}}$ values of ~2-3‰ at the beginning of MIS 5.4, of ~3.5-4.5‰ at
535 the beginning of MIS 4, and the concurrent increases in m_{terr} (Figure 6) might be
536 explained (i) by a higher contribution of (^{15}N -depleted) terrestrial organic matter, or (ii)
537 by stronger vertical mixing. We disregard the first possibility, because we already
538 discarded the potential effect of terrestrial nitrogen on the $\delta^{15}\text{N}_{\text{bulk}}$ signal (Section
539 5.1). Stronger vertical mixing in the Bering Sea during MIS 5.4 and 4 might be related
540 to the increased formation and/or ventilation of intermediate waters as inferred from
541 neodymium isotope ratios by Horikawa et al. (2010). The authors suggested that sea-
542 ice formation and according brine rejection led to the subduction of surface waters to
543 intermediate depths. Enhanced formation of sea-ice, acting as the transport agent for
544 terrestrial organic matter would be in accordance with this assumption and explain
545 the higher m_{terr} values. Other studies support the idea of well-ventilated intermediate
546 waters in the Bering Sea and North Pacific during glacial times (Ohkushi et al., 2003;
547 Itaki et al., 2009; Kim et al., 2011) and during severe stadial episodes (Rella et al.,
548 2012). The enhanced formation and/or ventilation of intermediate waters at the end
549 of MIS 6 and during the LGM implied by the record of Horikawa et al. (2010) is not
550 reflected in our $\delta^{15}\text{N}_{\text{bulk}}$ record, which rather suggests strong stratification during that

551 time. However, these observations are not necessarily contradictory, since
552 intermediate waters could have been formed outside the still-stratified Bering Sea. In
553 fact, recent reconstructions of past ventilation changes in the subarctic North Pacific
554 using radiocarbon-derived ventilation ages in combination with epibenthic stable
555 carbon isotope ratios point to the Okhotsk Sea as the source region of intermediate
556 waters during HS1 and the YD (Max et al., 2014).

557 In addition to insolation forcing, sea-level changes might have influenced the extent
558 of stratification in the Bering Sea. Today, the only shallow (~50 m) Bering Strait
559 allows for oceanic communication between the North Pacific and the N Atlantic.
560 During glacial times the closed Bering Strait prevented the flux of relatively fresh
561 waters into the Atlantic, which is thought to have affected the Atlantic meridional
562 overturning circulation (Hu et al., 2010). Lower glacial sea-level is also likely to have
563 reduced the inflow of Alaskan Stream waters into the Bering Sea (Gorbarenko et al.,
564 2005; Tanaka and Takahashi, 2005). As suggested by relative sea-level
565 reconstructions (e.g., Waelbroeck et al., 2002; Yokoyama and Esat, 2011), the
566 Bering Strait was closed during MIS 6 and in between MIS 4 to 2 until ~12-11 ka BP
567 (Keigwin et al., 2006) (Figure 6). Our $\delta^{15}\text{N}_{\text{bulk}}$ values indicate almost complete nitrate
568 utilization during late MIS 6 (~150-130 ka BP) and during MIS 3 and 2 as a result of
569 strong stratification. During this time a closed Bering Strait is likely to have fostered
570 stratification due to the pooling of the relatively fresh waters within the Bering Sea,
571 which would have resulted in a strengthened pycnocline. Support for this view and for
572 fresher glacial conditions in the Bering Sea comes from diatom and radiolarian
573 assemblages (Sancetta, 1983; Katsuki and Takahashi, 2005; Tanaka and Takahashi,
574 2005). Notably, during MIS 3 and 2 the $\delta^{15}\text{N}_{\text{bulk}}$ values recorded at Shirshov Ridge
575 are on average ~1‰ lower than at Bowers Ridge Site 17JPC and ~0.5‰ lower than
576 at Site PC24A (Figure 7). This might indicate that stratification in the Bering Sea was
577 regionally different and more pronounced in the South, or that influence from
578 denitrification resulted in the heavier $\delta^{15}\text{N}$ values.

579

580

581

582 5.3 Deglacial and interglacial conditions

583 In our records, the deglaciations are characterized by the transition from the glacial
584 situation of pronounced stratification with almost complete nitrate utilization and low
585 export production toward the interglacial situation of reduced stratification, high
586 marine productivity, and reduced terrestrial input. Yet, Termination II and Termination
587 I show some notable differences. During Termination I our $\delta^{15}\text{N}_{\text{bulk}}$ record is
588 characterized by an initial decrease, which might correspond to the HS1 cold phase,
589 subsequent local maxima during the B/A and the early Holocene warm phases, and
590 an intercalated minimum during the YD (Figure 6). The same temporal evolution was
591 reported for sedimentary and diatom-bound $\delta^{15}\text{N}$ at Bering Sea sites 17JPC (Brunelle
592 et al., 2007, 2010) and PC24A (Kim et al., 2011). The B/A-peak, occurring
593 simultaneously with a rise in export production, is found in several other records from
594 the North Pacific realm and related to enhanced denitrification (Keigwin et al., 1992;
595 Emmer and Thunell, 2000; Ternois et al., 2001; Kienast et al., 2002; Galbraith et al.,
596 2008a; Kao et al., 2008; Brunelle et al., 2007, 2010; Addison et al., 2012; Khim et al.,
597 2012; Schlung et al., 2013).

598 Notably, m_{terr} shows a local maximum during HS1 at Site 85KL. Hence, the initial
599 decrease in $\delta^{15}\text{N}_{\text{bulk}}$ might be related to higher terrestrial input or to lower nitrate
600 utilization due to weakened stratification. However, the latter should have resulted in
601 higher export production, which is not observed at our site. This drop is not fully
602 understood and alternative explanations include changes in $\delta^{15}\text{N}_{\text{nitrate}}$, iron limitation,
603 and light limitation (Brunelle et al., 2007, 2010; Lam et al., 2013). Light limitation by
604 expanded sea-ice coverage is supported by the qualitative detection of IP_{25} in
605 western Bering Sea sediments during HS1 and the YD (Max et al., 2012).

606 During the B/A and the early Holocene our $\delta^{15}\text{N}_{\text{bulk}}$ values exceeded the modern
607 $\delta^{15}\text{N}_{\text{nitrate}}$ value, supporting an increase in denitrification. At the same time a shift
608 toward oxygen-depleted bottom water conditions is inferred from benthic foraminiferal
609 assemblages (Kim et al., 2011; Ovsepyan et al., 2013), which is in agreement with
610 the proposed expansion of the OMZ and the occurrence of laminated sediments
611 during warm intervals (e.g., Zheng et al., 2000; van Geen et al., 2003; Cook et al.,
612 2005; Kuehn et al., 2014). A recent comparison between alkenone- and Mg/Ca-

613 based paleotemperature estimates suggests enhanced thermal mixed-layer
614 stratification in the western Bering Sea during the B/A (Riethdorf et al., 2013b),
615 implying that at least some of the recorded $\delta^{15}\text{N}_{\text{bulk}}$ increase is due to stronger
616 surface nitrate utilization. Recently, Lam et al. (2013) suggested two stepwise events
617 starting with deep convection initialized at ~ 18 ka BP increasing the nutrient supply
618 but inducing light limitation, and subsequent meltwater-induced stratification resulting
619 in bloom conditions and leaving surface waters enriched in nutrients. The drop in
620 $\delta^{15}\text{N}_{\text{bulk}}$ observed during the YD in hand with decreasing SSTs and the presence of
621 IP_{25} (Max et al., 2012) argues for a similar situation as recorded during HS1.

622 Termination II differs from Termination I at Site 85KL in such that the $\delta^{15}\text{N}_{\text{bulk}}$ values
623 are lower and presumably not affected by denitrification. An early deglacial $\delta^{15}\text{N}_{\text{bulk}}$
624 minimum at ~ 133 ka BP, followed by a local maximum at ~ 131 ka BP might hint
625 toward analogs of the HS1 and the B/A, respectively. The subsequent drop in $\delta^{15}\text{N}_{\text{bulk}}$
626 into MIS 5.5 reflecting the 'breakdown' of glacial stratification is sudden and
627 accompanied by the decrease in both, m_{terr} and bottom water oxygenation then
628 prevailing during the penultimate interglacial (Figure 6). Notably, this drop from
629 relatively high MIS 6 values occurred ~ 5 kyr before the maximum in insolation was
630 reached, but its timing is comparable to that recorded in the NW Pacific. In the
631 Okhotsk Sea it seems to have occurred significantly earlier at ~ 147 - 141 ka BP
632 (Figure 7). A respective drop in $\delta^{15}\text{N}_{\text{bulk}}$ during Termination I was not recorded at Site
633 85KL until ~ 9.1 ka BP, while at Bowers Ridge sites U1340 (Schlung et al., 2013) and
634 17JPC (Brunelle et al., 2007) it occurred directly after the B/A maximum.

635

636 **5.4 Millennial-scale oscillations**

637 Riethdorf et al. (2013a) reported on millennial-scale oscillations in core 85KL, thought
638 to reflect increased export production and sudden sea-ice melt, which might be
639 connected to GI (Dansgaard-Oeschger events; e.g., Dansgaard et al., 1993). Similar
640 observations are reported for other sediment cores from the Bering Sea (Gorbarenko
641 et al., 2005, 2010b; Kim et al., 2011; Rella et al., 2012; Schlung et al., 2013) and the
642 Okhotsk Sea (Gorbarenko et al., 2007, 2010a, 2012), indicating warmer SSTs,
643 enhanced marine productivity, weak ventilation of intermediate waters, and poor

644 (dysoxic) dissolved oxygen conditions during interstadials. NE Pacific sediments
645 related to GI are in part laminated and suggested to reflect phases of weak
646 ventilation of NPIW and fluctuations in the strength of the OMZ (Behl and Kennett,
647 1996; Cannariato and Kennett, 1999; Hendy and Kennett, 2000, 2003). Results of
648 Ortiz et al. (2004) from a core off Baja California implied that elevated marine
649 productivity was caused by enhanced nutrient flux to surface waters.

650 In the Bering Sea higher interstadial $\delta^{15}\text{N}_{\text{bulk}}$ values were explained by Kim et al.
651 (2011) by increased marine productivity as a result of reduced sea-ice influence and
652 a strengthened BSC. They also suggested that stronger inflow of water masses from
653 the Gulf of Alaska (Gorbarenko et al., 2005) resulted in enhanced nutrient supply to
654 Bering Sea surface waters. Schlung et al. (2013) attributed higher $\delta^{15}\text{N}_{\text{bulk}}$ and
655 concurrent minima in planktonic $\delta^{13}\text{C}$ to amplified local upwelling of subsurface
656 nitrate rather than to increased nitrate utilization. Our data show short-lived maxima
657 in $\delta^{15}\text{N}_{\text{bulk}}$ and concurrent minima in m_{terr} during some, but not all, GI (1, 7, 8, 12, 17-
658 20), and during MIS 6 (at ~133, ~148, and ~173 ka BP) when export production was
659 high (Figure 6). The opposite pattern was recorded when export production was low
660 during some GS (2, 7, 18, 20) and also during MIS 6 (at ~151, ~157, and ~170 ka
661 BP). Despite the low reproducibility of our $\delta^{15}\text{N}_{\text{bulk}}$ results our data support the view of
662 increased interstadial marine productivity which led to stronger utilization of the
663 available nitrate in a still stratified upper water column. During interstadials warmer
664 SSTs most probably resulted in less sea-ice influence and reduced supply of
665 terrestrial organic matter. Conversely, during stadials strengthened sea-ice formation
666 and coverage is likely to have restricted marine productivity, led to enhanced
667 terrestrial organic matter supply to Bering Sea sediments, and resulted in better
668 ventilation of NPIW, potentially making the Bering Sea a proximate source of this
669 water mass as suggested by Rella et al. (2012).

670

671 **6. Summary**

672 We determined TN, TOC, $\delta^{13}\text{C}_{\text{bulk}}$ and $\delta^{15}\text{N}_{\text{bulk}}$ in a core from the western Bering Sea
673 in high-resolution to reconstruct changes in surface nitrate utilization (stratification)
674 over the last 180 kyr. A linear endmember model was applied to assess the

675 contributions of marine- and terrestrial-derived organic matter. Besides the expected
676 difference between glacial and interglacial conditions reported for the subarctic NW
677 Pacific and its marginal seas, our results suggest a more complex evolution of
678 stratification with enhanced vertical mixing during warm intervals (MIS 5.5, 5.3, 5.1,
679 1), and stratification becoming fostered during cold intervals (MIS 6, 5.4, 5.2, 4-2).
680 This development is explained by insolation forcing and a feedback in sea-ice
681 formation and the strength of winter mixing. In addition, sea-level changes might
682 have further influenced the extent of stratification when the Bering Strait was closed
683 and relatively fresh waters pooled in the Bering Sea. During warm intervals,
684 variations in seasonal contrasts, sea-ice influence, and stratification resulted in
685 enhanced export production and dominantly marine-derived organic matter, but less
686 nitrate utilization due to better vertical mixing. Conversely, enhanced terrestrial-
687 derived organic matter, most probably associated with sea-ice formation, low export
688 production, and enhanced stratification characterized cold intervals of the past 180
689 kyr. Moreover, we present supporting evidence that millennial-scale climate
690 oscillations connected with Greenland interstadials occurred in the Bering Sea
691 environment, and that sea-ice formation there influenced the ventilation of North
692 Pacific Intermediate Water.

693

694 **Acknowledgements**

695 Financial support for this study was provided by a Japan Society for the Promotion of
696 Science (JSPS) short-term postdoctoral fellowship to J.-R.R. (grant no. PE12528).
697 Additional support came from the "Funding Program for Next Generation World-
698 Leading Researchers (NEXT Program GR031)" of JSPS, initiated by the Council for
699 Science and Technology Policy (CSTP), awarded to Y.Y. Core 85KL was recovered
700 in the framework of the joint German-Russian research project KALMAR, funded by
701 the German Federal Ministry of Education and Research (BMBF, grant nos.
702 03G0672A and B). We thank N. Ohkouchi, N. Harada, Y. Okazaki, and H. Vollstaedt
703 for helpful discussions, as well as Christina Ravelo and the anonymous reviewer for
704 their fruitful comments that improved the manuscript. Supplementary data are

705 available via the PANGAEA Data Publisher for Earth & Environmental Science
706 (<http://doi.pangaea.de/10.1594/PANGAEA.807383>).

707

708 **References**

709 Addison, J.A., Finney, B.P., Dean, W.E., Davies, M.H., Mix, A.C., Stoner, J.S.,
710 Jaeger, J.M., 2012. Productivity and sedimentary $\delta^{15}\text{N}$ variability for the last 17,000
711 years along the northern Gulf of Alaska. *Paleoceanography* 27, PA1206.
712 doi:10.1029/2011PA002161.

713 Altabet, M.A., Francois, R., 1994. Sedimentary nitrogen isotopic ratio as a recorded
714 for surface ocean nitrate utilization. *Global Biogeochem. Cy.* 8 (1), 103-116.

715 Altabet, M.A., Pilskaln, C., Thunell, R., Pride, C., Sigman, D., Chavez, F., Francois,
716 R., 1999. The nitrogen isotope biogeochemistry of sinking particles from the margin
717 of the Eastern North Pacific. *Deep-Sea Res. Pt. I* 46, 655-679.

718 Asahara, Y., Takeuchi, F., Nagashima, K., Harada, N., Yamamoto, K., Oguri, K.,
719 Tadai, O., 2012. Provenance of terrigenous detritus of the surface sediments in the
720 Bering and Chukchi Seas as derived from Sr and Nd isotopes: Implications for recent
721 climate change in the Arctic regions. *Deep-Sea Res. Pt. II* 61-64, 155-171.
722 doi:10.1016/j.dsr2.2011.12.004.

723 Barford, C.C., Montoya, J.P., Altabet, M.A., Mitchell, R., 1999. Steady-state nitrogen
724 isotope effects of N_2 and N_2O production in *Paracoccus denitrificans*. *Appl. Environ.*
725 *Microb.* 65 (3), 989-994.

726 Behl, R.J., Kennett, J.P., 1996. Brief interstadial events in the Santa Barbara basin,
727 NE Pacific, during the past 60 kyr. *Nature* 379, 243-246.

728 Blockley, S.P.E., Lane, C.S., Hardiman, M., Rasmussen, S.O., Seierstad, I.K.,
729 Steffensen, J.P., Svensson, A., Lotter, A.F., Turney, C.S.M., Ramsey, C.B.,
730 INTIMATE members, 2012. Synchronisation of palaeoenvironmental records over the
731 last 60,000 years, and an extended INTIMATE event stratigraphy to 48,000 b2k.
732 *Quaternary Sci. Rev.* 36, 2-10. doi:10.1016/j.quascirev.2011.09.017.

- 733 Brodie, C.R., Casford, J.S.L., Lloyd, J.M., Leng, M.J., Heaton, T.H.E., Kendrick, C.P.,
734 Yongqiang, Z., 2011a. Evidence for bias in C/N, $\delta^{13}\text{C}$ and $\delta^{15}\text{N}$ values of bulk organic
735 matter, and on environmental interpretation, from a lake sedimentary sequence by
736 pre-analysis acid treatment methods. *Quaternary Sci. Rev.* 30, 3076-3087.
737 doi:10.1016/j.quascirev.2011.07.003.
- 738 Brodie, C.R., Heaton, T.H.E., Leng, M.J., Kendrick, C.P., Casford, J.S.L., Lloyd, J.M.,
739 2011b. Evidence for bias in measured $\delta^{15}\text{N}$ values of terrestrial and aquatic organic
740 materials due to pre-analysis acid treatment methods. *Rapid Commun. Mass Sp.* 25,
741 1089-1099. doi:10.1002/rcm.4970.
- 742 Brunelle, B.G., Sigman, D.M., Cook, M.S., Keigwin, L.D., Haug, G.H., Plessen, B.,
743 Schettler, G., Jaccard, S.L., 2007. Evidence from diatom-bound nitrogen isotopes for
744 subarctic Pacific stratification during the last ice age and a link to North Pacific
745 denitrification changes. *Paleoceanography* 22, PA1215. doi:10.1029/2005PA001205.
- 746 Brunelle, B.G., Sigman, D.S., Jaccard, S.L., Keigwin, L.D., Plessen, B., Schettler, G.,
747 Cook, M.S., Haug, G.H., 2010. Glacial/interglacial changes in nutrient supply and
748 stratification in the western subarctic North Pacific since the penultimate glacial
749 maximum. *Quaternary Sci. Rev.* 29, 2579-2590.
750 doi:10.1016/j.quascirev.2010.03.010.
- 751 Cannariato, K.G., Kennett, J.P., 1999. Climatically related millennial-scale
752 fluctuations in strength of California margin oxygen-minimum zone during the past 60
753 k.y.. *Geology* 27 (11), 975-978.
- 754 Carpenter, E.J., Harvey, H.R., Fry, B., Capone, D.G., 1997. Biogeochemical tracers
755 of the marine cyanobacterium *Trichodesmium*. *Deep-Sea Res. Pt. I* 44 (1), 27-38.
- 756 Chikamoto, M.O., Menviel, L., Abe-Ouchi, A., Ohgaito, R., Timmermann, A., Okazaki,
757 Y., Harada, N., Oka, A., Mouchet, A., 2012. Variability in North Pacific intermediate
758 and deep water ventilation during Heinrich events in two coupled climate models.
759 *Deep-Sea Res. Pt. II* 61-64, 114-126. doi:10.1016/j.dsr2.2011.12.002.
- 760 Codispoti, L.A., Brandes, J.A., Christensen, J.P., Devol, A.H., Naqvi, S.W.A., Paerl,
761 H.W., Yoshinari, T., 2001. The oceanic fixed nitrogen and nitrous oxide budgets:
762 Moving targets as we enter the anthropocene?. *Sci. Mar.* 65 (Suppl. 2), 85-105.

- 763 Cook, M.S., Keigwin, L.D., Sancetta, C.A., 2005. The deglacial history of surface and
764 intermediate water of the Bering Sea. *Deep-Sea Res. Pt. II* 52, 2163-2173.
765 doi:10.1016/j.dsr2.2005.07.004.
- 766 Crusius, J., Pedersen, T.F., Kienast, S., Keigwin, L., Labeyrie, L., 2004. Influence of
767 northwest Pacific productivity on North Pacific Intermediate Water oxygen
768 concentrations during the Bolling-Allerod interval (14.7--12.9 ka). *Geology* 32 (7),
769 633-663. doi: 10.1130/G20508.1.
- 770 Dansgaard, W., Johnsen, S.J., Clausen, H.B., Dahl-Jensen, D., Gundestrup, N.S.,
771 Hammer, C.U., Hvidberg, C.S., Steffensen, J.P., Sveinbjörnsdottir, A.E., Jouzel, J.,
772 Bond, G., 1993. Evidence for general instability of past climate from a 250-kyr ice-
773 core record. *Nature* 364, 218-220.
- 774 Debret, M., Desmet, M., Balsam, W., Copard, Y., Francus, P., Laj, C., 2006.
775 Spectrophotometer analysis of Holocene sediments from an anoxic fjord: Saanich
776 Inlet, British Columbia, Canada. *Mar. Geol.* 229, 15-28.
777 doi:10.1016/j.margeo.2006.01.005.
- 778 Dullo, W.-C., Baranov, B., van den Bogaard, C. (Eds.), 2009. FS Sonne
779 Fahrtbericht/Cruise Report SO201-2 KALMAR, Busan/Korea-Tomakomai/Japan,
780 30.08.-08.10.2009. IFM-GEOMAR Report 35, Leibniz Institute of Marine Sciences,
781 Kiel, 233 pp.
- 782 Elderfield, H., Rickaby, R.E.M., 2000. Oceanic Cd/P ratio and nutrient utilization in
783 the glacial Southern Ocean. *Nature* 405, 305-310.
- 784 Emile-Geay, J., Cane, M., Naik, N., Seager, R., Clement, A.C., van Geen, A., 2003.
785 Warren revisited: Atmospheric freshwater fluxes and "Why is no deep water formed
786 in the North Pacific". *J. Geophys. Res.* 108 (C6), 3178. doi:10.1029/2011JC001058.
- 787 Emmer, E., Thunell, R.C., 2000. Nitrogen isotope variations in Santa Barbara Basin
788 sediments: Implications for denitrification in the eastern tropical North Pacific during
789 the last 50,000 years. *Paleoceanography* 15 (4), 377-387.
790 doi:10.1029/1999PA000417.
- 791 Francois, R., Altabet, M.A., Yu, E.-F., Sigman, D.M., Bacon, M.P., Frank, M.,
792 Bohrmann, G., Bareille, G., Labeyrie, L.D., 1997. Contribution of Southern Ocean

- 793 surface-water stratification to low atmosphere CO₂ concentrations during the last
794 glacial period. *Nature* 389, 929-935.
- 795 Galbraith, E.D., Kienast, M., Pedersen, T.F., Calvert, S.E., 2004. Glacial-interglacial
796 modulation of the marine nitrogen cycle by high-latitude O₂ supply to the global
797 thermocline. *Paleoceanography* 19, PA4007. doi:10.1029/2003PA001000.
- 798 Galbraith, E.D., Kienast, M., Jaccard, S.L., Pedersen, T.F., Brunelle, B.G., Sigman,
799 D.M., Kiefer, T., 2008a. Consistent relationship between global climate and surface
800 nitrate utilization in the western subarctic Pacific throughout the last 500 ka.
801 *Paleoceanography* 23, PA2212. doi:10.1029/2007PA001518.
- 802 Galbraith, E.D., Sigman, D.M., Robinson, R.S., Pedersen, T.F., 2008b. Nitrogen in
803 past marine environments, in: Capone, D.G., Bronk, D.A., Mulholland, M.R.,
804 Carpenter, E.J. (Eds.), *Nitrogen in the Marine Environment*. Second Edition, Elsevier
805 Inc., pp. 1497-1535. doi:10.1016/B978-0-12-372522-6.00034-7.
- 806 Garcia, H.E., Locarnini, R.A., Boyer, T.P., Antonov, J.I., 2010. *World Ocean Atlas*
807 2009, Volume 4: Nutrients (phosphate, nitrate, and silicate), in: Levitus, S. (Ed.),
808 *NOAA Atlas NESDIS 71*. U.S. Government Printing Office, Washington, D.C., 184
809 pp.
- 810 Gaye-Haake, B., Lahajnar, N., Emeis, K.-Ch., Unger, D., Rixen, T., Suthhof, A.,
811 Ramaswamy, V., Schulz, H., Paropkari, A.L., Guptha, M.V.S., Ittekkot, V., 2005.
812 Stable nitrogen isotopic ratios of sinking particles and sediments from the northern
813 Indian Ocean. *Mar. Chem.* 96, 243-255. doi:10.1016/j.marchem.2005.02.001.
- 814 Geider, R.J., La Roche, J., 2002. Redfield revisited: variability of C:N:P in marine
815 microalgae and its biochemical basis. *Eur. J. Phycol.* 37, 1-17.
816 doi:10.1017/S0967026201003456.
- 817 Goñi, M.A., Ruttenberg, K.C., Eglinton, T.I., 1998. A reassessment of the sources
818 and importance of land-derived organic matter in surface sediments from the Gulf of
819 Mexico. *Geochim. Cosmochim. Ac.* 62 (18), 3055-3075.
- 820 Gorbarenko, S.A., Khusid, T.A., Basov, I.A., Oba, T., Southon, J.R., Koizumi, I.,
821 2002. Glacial Holocene environment of the southeastern Okhotsk Sea: Evidence

- 822 from geochemical and palaeontological data. *Palaeogeogr. Palaeocl.* 177, 237-263.
823 doi:10.1016/S0031-0182(01)00335-2.
- 824 Gorbarenko, S.A., Basov, I.A., Chekhovskaya, M.P., Southon, J., Khusid, T.A.,
825 Artemova, A.V., 2005. Orbital and millennium scale environmental changes in the
826 southern Bering Sea during the last glacial-Holocene: Geochemical and
827 paleontological evidence. *Deep-Sea Res. Pt. II* 52, 2174-2185.
828 doi:10.1016/j.dsr2.2005.08.005.
- 829 Gorbarenko, S.A., Goldberg, E.L., Kashgarian, M., Velivetskaya, T.A., Zakharkov,
830 S.P., Pechnikov, V.S., Bosin, A.A., Psheneva, O.Y., Ivanova, E.D., 2007. Millennium
831 scale environment changes of the Okhotsk Sea during last 80 kyr and their phase
832 relationship with global climate changes. *J. Oceanogr.* 63, 609-623.
- 833 Gorbarenko, S.A., Harada, N., Malakhov, M.I., Vasilenko, Y.P., Bosin, A.A.,
834 Goldberg, E.L., 2010a. Orbital and millennial-scale environmental and
835 sedimentological changes in the Okhotsk Sea during the last 350 kyr. *Global Planet.*
836 *Change* 72, 79-85. doi:10.1016/j.gloplacha.2010.03.002.
- 837 Gorbarenko, S.A., Wang, P., Wang, R., Cheng, X., 2010b. Orbital and suborbital
838 environmental changes in the southern Bering Sea during the last 50 kyr.
839 *Palaeogeogr. Palaeocl.* 286, 97-106. doi:10.1016/j.palaeo.2009.12.014.
- 840 Gorbarenko, S.A., Harada, N., Malakhov, M.I., Velivetskaya, T.A., Vasilenko, Y.P.,
841 Bosin, A.A., Derkachev, A.N., Goldberg, E.L., Ignatiev, A.V., 2012. Responses of the
842 Okhotsk Sea environment and sedimentology to global climate changes at the orbital
843 and millennial scale during the last 350 kyr. *Deep-Sea Res. Pt. II* 61-64, 73-84.
844 doi:10.1016/j.dsr2.2011.05.016.
- 845 Guo, L., Macdonald, R.W., 2006. Source and transport of terrigenous organic matter
846 in the upper Yukon River: Evidence, from isotopic ($\delta^{13}\text{C}$, $\Delta^{14}\text{C}$, and $\delta^{15}\text{N}$) composition
847 of dissolved, colloidal, and particulate phases. *Global Biogeochem. Cy.* 20, GB2011.
848 doi:10.1029/2005GB002593.
- 849 Guo, L., Tanaka, T., Wang, D., Tanaka, N., Murata, A., 2004. Distributions,
850 speciation and stable isotope composition of organic matter in the southeastern
851 Bering Sea. *Mar. Chem.* 91, 211-226. doi:10.1016/j.marchem.2004.07.002.

- 852 Haug, G.H., Sigman, D.M., Tiedemann, R., Pedersen, T.F., Sarinthein, M., 1999.
853 Onset of permanent stratification in the subarctic Pacific Ocean. *Nature* 401, 779-
854 782.
- 855 Hendy, I.L., Kennett, J.P., 2000. Dansgaard-Oeschger cycles and the California
856 Current System: Planktonic foraminiferal response to rapid climate change in Santa
857 Barbara Basin, Ocean Drilling Program hole 893A. *Paleoceanography* 15 (1), 30-42.
- 858 Hendy, I.L., Kennett, J.P., 2003. Tropical forcing of North Pacific intermediate water
859 distribution during Late Quaternary rapid climate change? *Quaternary Sci. Rev.* 22,
860 673-689. doi:10.1016/S0277-3791(02)00186-5.
- 861 Honda, M.C., Imai, K., Nojiri, Y., Hoshi, F., Sugawara, T., Kusakabe, M., 2002. The
862 biological pump in the northwestern North Pacific based on fluxes and major
863 components of particulate matter obtained by sediment-trap experiments (1997-
864 2000). *Deep-Sea Res. Pt. II* 49, 5595-5625. doi:10.1016/S0967-0645(02)00201-1.
- 865 Horikawa, K., Asahara, Y., Yamamoto, K., Okazaki, Y., 2010. Intermediate water
866 formation in the Bering Sea during glacial periods: Evidence from neodymium isotope
867 ratios. *Geology* 38 (5), 435-438. doi:10.1130/G30225.1.
- 868 Hu, A., Meehl, G.A., Otto-Bliesner, B.L., Waelbroeck, C., Han, W., Loutre, M.-F.,
869 Lambeck, K., Mitrovica, J.X., Rosenbloom, N., 2010. Influence of Bering Strait flow
870 and North Atlantic circulation on glacial sea-level changes. *Nat. Geosci.* 3, 118-121.
871 doi:10.1038/ngeo0729.
- 872 Itaki, T., Uchida, M., Kim, S., Shin, H.-S., Tada, R., Khim, B.-K., 2009. Late
873 Pleistocene stratigraphy and palaeoceanographic implications in northern Bering Sea
874 slope sediments: Evidence from the radiolarian species *Cycladophora davisiana*. *J.*
875 *Quaternary Sci.* 24 (8), 856-865. doi:10.1002/jqs.1356.
- 876 Jaccard, S.L., Galbraith, E.D., 2012. Large climate-driven changes of oceanic oxygen
877 concentrations during the last deglaciation. *Nat. Geosci.* 5 (2), 151-156.
878 doi:10.1038/ngeo1352.
- 879 Jaccard, S.L., Galbraith, E.D., 2013. Direct ventilation of the North Pacific did not
880 reach the deep ocean during the last deglaciation. *Geophys. Res. Lett.* 40, 199-203.
881 doi:10.1029/2012GL054118.

- 882 Jaccard, S.L., Haug, G.H., Sigman, D.M., Pedersen, T.F., Thierstein, H.R., Röhl, U.,
883 2005. Glacial/interglacial changes in subarctic North Pacific stratification. *Science*
884 308, 1003-1006. doi:10.1126/science.1108696.
- 885 Jaccard, S.L., Galbraith, E.D., Sigman, D.M., Haug, G.H., 2010. A pervasive link
886 between Antarctic ice core and subarctic Pacific sediment records over the past 800
887 kyrs. *Quaternary Sci. Rev.* 29, 206-212. doi:10.1016/j.quascirev.2009.10.007.
- 888 Kao, S.J., Liu, K.K., Hsu, S.C., Chang, Y.P., Dai, M.H., 2008. North Pacific-wide
889 spreading of isotopically heavy nitrogen during the last deglaciation: Evidence from
890 the western Pacific. *Biogeosciences* 5, 1641-1650. doi:10.5194/bg-5-1641-2008.
- 891 Kashiyama, Y., Ogawa, N.O., Shiro, M., Tada, R., Kitazato, H., Ohkouchi, N., 2008.
892 Reconstruction of the biogeochemistry and ecology of photoautotrophs based on the
893 nitrogen and carbon isotopic compositions of vanadyl porphyrins from Miocene
894 siliceous sediments. *Biogeosciences* 5, 797-816. doi:10.5194/bg-5-797-2008.
- 895 Katsuki, K., Takahashi, K., 2005. Diatoms as paleoenvironmental proxies for
896 seasonal productivity, sea-ice and surface circulation in the Bering Sea during the
897 late Quaternary. *Deep-Sea Res. Pt. II* 52, 2110-2130.
898 doi:10.1016/j.dsr2.2005.07.001.
- 899 Keigwin, L.D., Jones, G.A., Froelich, P.N., 1992. A 15,000 year paleoenvironmental
900 record from Meiji Seamount, far northwestern Pacific. *Earth Planet. Sc. Lett.* 111,
901 425-440.
- 902 Keigwin, L.D., Donnelly, J.P., Cook, M.S., Driscoll, N.W., Brigham-Grette, J., 2006.
903 Rapid sea-level rise and Holocene climate in the Chukchi Sea. *Geology* 34 (10), 861-
904 864. doi:10.1130/G22712.1.
- 905 Khim, B.-K., Sakamoto, T., Harada, N., 2012. Reconstruction of surface water
906 conditions in the central region of the Okhotsk Sea during the last 180 kyrs. *Deep-*
907 *Sea Res. Pt. II* 61-64, 63-72. doi:10.1016/j.dsr2.2011.05.014.
- 908 Kienast, S.S., Calvert, S.E., Pedersen, T.F., 2002. Nitrogen isotope and productivity
909 variations along the northeast Pacific margin over the last 120 kyr: Surface and
910 subsurface paleoceanography. *Paleoceanography* 17 (4), 1055.
911 doi:10.1029/2001PA000650.

- 912 Kienast, S.S., Hendy, I.L., Crusius, J., Pedersen, T.F., Calvert, S.E., 2004. Export
913 production in the subarctic North Pacific over the last 800 kyrs: No evidence for iron
914 fertilization? *J. Oceanogr.* 60 (1), 189-203.
- 915 Kim, S., Khim, B.K., Uchida, M., Itaki, T., Tada, R., 2011. Millennial-scale
916 paleoceanographic events and implication for the intermediate-water ventilation in
917 the northern slope area of the Bering Sea during the last 71 kyrs. *Global Planet.*
918 *Change* 79, 89-98. doi:10.1016/j.gloplacha.2011.08.004.
- 919 Kuehn, H., Lembke-Jene, L., Gersonde, R., Esper, O., Lamy, F., Arz, H., Tiedemann,
920 R., 2014. Laminated sediments in the Bering Sea reveal atmospheric teleconnections
921 to Greenland climate on millennial to decadal timescales during the last
922 deglaciations. *Clim. Past Discuss.* 10, 2467-2518. doi:10.5194/cpd-10-2467-2014.
- 923 Lam, P.J., Robinson, L.F., Blusztajn, J., Li, C., Cook, M.S., McManus, J.F., Keigwin,
924 L.D., 2013. Transient stratification as the cause of the North Pacific productivity spike
925 during deglaciation. *Nat. Geosci.* 6, 622-626. doi:10.1038/ngeo1873.
- 926 Laskar, J., Robutel, P., Joutel, F., Gastineau, M., Correia, A.C.M., Levrard, B., 2004.
927 A long-term numerical solution for the insolation quantities of the Earth. *Astron.*
928 *Astrophys.* 428, 261-285. doi:10.1051/0004-6361:20041335.
- 929 Lehmann, M.F., Sigman, D.M., McCorkle, D.C., Brunelle, B.G., Hoffmann, S.,
930 Kienast, M., Cane, G., Clement, J., 2005. Origin of the deep Bering Sea nitrate
931 deficit: Constraints from the nitrogen and oxygen isotopic composition of water
932 column nitrate and benthic nitrate fluxes. *Global Biogeochem. Cy.* 19, GB4005.
933 doi:10.1029/2005GB002508.
- 934 Lisiecki, L.E., Raymo, M.E., 2005. A Pliocene-Pleistocene stack of 57 globally
935 distributed benthic $\delta^{18}\text{O}$ records. *Paleoceanography* 20, PA1003.
936 doi:10.1029/2004PA001071.
- 937 Liu, K.-K., Kaplan, I.R., 1989. The eastern tropical Pacific as a source of ^{15}N -enriched
938 nitrate in seawater off southern California. *Limnol. Oceanogr.* 34 (5), 820-830.
- 939 Macdonald, A.M., Suga, T., Curry, R.G., 2001. An isopycnally averaged North Pacific
940 climatology. *J. Atmos. Ocean. Tech.* 18 (3), 394-420.

- 941 Mariotti, A., Germon, J.C., Hubert, P., Kaiser, P., Letolle, R., Tardieux, A., Tardieux,
942 P., 1981. Experimental determination of nitrogen kinetic isotope fractionation: Some
943 principles; Illustration for the denitrification and nitrification processes. *Plant Soil* 62
944 (3), 413-430. doi:10.1007/BF02374138.
- 945 Matsumoto, K., Oba, T., Lynch-Stieglitz, J., Yamamoto, H., 2002. Interior
946 hydrography and circulation of the glacial Pacific Ocean. *Quaternary Sci. Rev.* 21,
947 1693-1704. doi:10.1016/S0277-3791(01)00142-1.
- 948 Max, L., Riethdorf, J.-R., Tiedemann, R., Smirnova, M., Lembke-Jene, L., Fahl, K.,
949 Nürnberg, D., Matul, A., Mollenhauer, G., 2012. Sea surface temperature variability
950 and sea-ice extent in the subarctic northwest Pacific during the past 15,000 years.
951 *Paleoceanography* 27, PA3213. doi:10.1029/2012PA002292.
- 952 Max, L., Lembke-Jene, L., Riethdorf, J.-R., Tiedemann, R., Nürnberg, D., Kühn, H.,
953 Mackensen, A., 2014. Pulses of enhanced North Pacific Intermediate Water
954 ventilation from the Okhotsk Sea and Bering Sea during the last deglaciation. *Clim.*
955 *Past* 10, 591-605. doi:10.5194/cp-10-591-2014.
- 956 McQuoid, M.R., Whiticar, M.J., Calvert, S.E., Pedersen, T.F., 2001. A post-glacial
957 isotope record of primary production and accumulation in the organic sediments of
958 Saanich Inlet, ODP Leg 169S. *Mar. Geol.* 174, 273-286.
- 959 Méheust, M., Fahl, K., Stein, R., 2013. Variability in modern sea surface temperature,
960 sea ice and terrigenous input in the sub-polar North Pacific and Bering Sea:
961 Reconstruction from biomarker data. *Org. Geochem.* 57, 54-64.
962 doi:10.1016/j.orggeochem.2013.01.008i.
- 963 Menviel, L., Timmermann, A., Elison Timm, O., Mouchet, A., Abe-Ouchi, A.,
964 Chikamoto, M.O., Harada, N., Ohgaito, R., Okazaki, Y., 2012. Removing the North
965 Pacific halocline: Effects on global climate, ocean circulation and the carbon cycle.
966 *Deep-Sea Res. Pt. II* 61-64, 106-113. doi:10.1016/j.dsr2.2011.03.005.
- 967 Meyers, P.A., 1994. Preservation of elemental and isotopic source identification of
968 sedimentary organic matter. *Chem. Geol.* 114, 289-302.

- 969 Müller, P.J., Schneider, R., 1993. An automated leaching method for the
970 determination of opal in sediments and particulate matter. *Deep-Sea Res. Pt. I* 40
971 (3), 425-444.
- 972 Nagashima, K., Asahara, Y., Takeuchi, F., Harada, N., Toyoda, S., Tada, R., 2012.
973 Contribution of detrital materials from the Yukon River to the continental shelf
974 sediments of the Bering Sea based on the electron spin resonance signal intensity
975 and crystallinity of quartz. *Deep-Sea Res. Pt. II* 61-64, 145-154.
976 doi:10.1016/j.dsr2.2011.12.001.
- 977 Nakatsuka, T., Watanabe, K., Handa, N., Matsumoto, E., 1995. Glacial to interglacial
978 surface nutrient variations of Bering deep basins recorded by $\delta^{13}\text{C}$ and $\delta^{15}\text{N}$ of
979 sedimentary organic matter. *Paleoceanography* 10 (6), 1047-1061.
- 980 Narita, H., Sato, M., Tsunogai, S., Murayama, M., Ikehara, M., Nakatsuka, T.,
981 Wakatsuchi, M., Harada, N., Ujiie, Y., 2002. Biogenic opal indicating less productive
982 northwestern North Pacific during the glacial ages. *Geophys. Res. Lett.* 29 (15),
983 1732. doi:10.1029/2001GL014320.
- 984 Needoba, J.A., Waser, N.A., Harrison, P.J., Calvert, S.E., 2003. Nitrogen isotope
985 fractionation in 12 species of marine phytoplankton during growth on nitrate. *Mar.*
986 *Ecol.-Prog. Ser.* 255, 81-91. doi:10.3354/meps255081.
- 987 Niebauer, H.J., Bond, N.A., Yakunin, L.P., Plotnikov, V.V., 1999. An update on the
988 climatology and sea ice of the Bering Sea, in: Loughlin, T.R., Ohtani, K. (Eds.),
989 *Dynamics of the Bering Sea*. University of Alaska Sea Grant, Fairbanks, Alaska, pp.
990 29-59.
- 991 North Greenland Ice Core Project members, 2004. High-resolution record of Northern
992 Hemisphere climate extending into the last interglacial period. *Nature* 431, 147-151.
993 doi:10.1038/nature02848.
- 994 Nürnberg, D., Tiedemann, R., 2004. Environmental change in the Sea of Okhotsk
995 during the last 1.1 million years. *Paleoceanography* 19, PA4011.
996 doi:10.1029/2004PA001023.
- 997 Nürnberg, D., Dethleff, D., Tiedemann, R., Kaiser, A., Gorbarenko, S.A., 2011.
998 Okhotsk Sea ice coverage and Kamchatka glaciation over the last 350 ka - Evidence

- 999 from ice-rafted debris and planktonic $\delta^{18}\text{O}$. *Palaeogeogr. Palaeoclimatol.* 310, 191-205.
1000 doi:10.1016/j.palaeo.2011.07.011.
- 1001 Ohkushi, K., Itaki, T., Nemoto, N., 2003. Last Glacial-Holocene change in
1002 intermediate-water ventilation in the Northwestern Pacific. *Quaternary Sci. Rev.* 22,
1003 1477-1484. doi:10.1016/S0277-3791(03)00082-9.
- 1004 Okazaki, Y., Takahashi, K., Asahi, H., Katsuki, K., Hori, J., Yasuda, H., Sagawa, Y.,
1005 Tokuyama, H., 2005a. Productivity changes in the Bering Sea during the late
1006 Quaternary. *Deep-Sea Res. Pt. II* 52, 2150-2162. doi:10.1016/j.dsr2.2005.07.003.
- 1007 Okazaki, Y., Takahashi, K., Katsuki, K., Ono, A., Hori, J., Sakamoto, T., Uchida, M.,
1008 Shibata, Y., Ikehara, M., Aoki, K., 2005b. Late Quaternary paleoceanographic
1009 changes in the southwestern Okhotsk Sea: Evidence from geochemical, radiolarian,
1010 and diatom records. *Deep-Sea Res. Pt. II* 52, 2332-2350.
1011 doi:10.1016/j.dsr2.2005.07.007.
- 1012 Okazaki, Y., Timmermann, A., Menviel, L., Harada, N., Abe-Ouchi, A., Chikamoto,
1013 M.O., Mouchet, A., Asahi, H., 2010. Deepwater formation in the North Pacific during
1014 the last glacial termination. *Science* 329, 200-204. doi:10.1126/science.1190612.
- 1015 Okazaki, Y., Sagawa, T., Asahi, H., Horikawa, K., Onodera, J., 2012. Ventilation
1016 changes in the western North Pacific since the last glacial period. *Clim. Past* 8, 17-
1017 24. doi:10.5194/cp-8-17-2012.
- 1018 Ortiz, J.D., O'Connell, S.B., DelViscio, J., Dean, W., Carriquiry, J.D., Marchitto, T.,
1019 Zheng, Y., van Geen, A., 2004. Enhanced marine productivity off western North
1020 America during warm climate intervals of the past 52 k.y.. *Geology* 32 (6), 521-524.
1021 doi:10.1130/G20234.1.
- 1022 Ovsepyan, E.A., Ivanova, E.V., Max, L., Riethdorf, J.-R., Nürnberg, D., Tiedemann,
1023 R., 2013. Late Quaternary oceanographic conditions in the western Bering Sea.
1024 *Oceanology* 53 (2), 211-222. doi:10.1134/S0001437013020136.
- 1025 Pennock, J.R., Velinsky, D.J., Ludlam, J.M., Sharp, J.H., Fogel, M.L., 1996. Isotopic
1026 fractionation of ammonium and nitrate during uptake by *Skeletonema costatum*:
1027 Implications for $\delta^{15}\text{N}$ dynamics under bloom conditions. *Limnol. Oceanogr.* 41 (3),
1028 451-459.

- 1029 Perdue, E.M., Koprivnjak, J.-F., 2007. Using the C/N ratio to estimate terrigenous
1030 inputs of organic matter to aquatic environments. *Estuar. Coast. Shelf S.* 73, 65-72.
1031 doi:10.1016/j.ecss.2006.12.021.
- 1032 Rasmussen, S.O., Andersen, K.K., Svensson, A.M., Steffensen, J.P., Vinther, B.M.,
1033 Clausen, H.B., Siggaard-Andersen, M.-L., Johnsen, S.J., Larsen, L.B., Dahl-Jensen,
1034 D., Bigler, M., Röthlisberger, R., Fischer, H., Goto-Azuma, K., Hansson, M.E., Ruth,
1035 U., 2006. A new Greenland ice core chronology for the last glacial termination. *J.*
1036 *Geophys. Res.* 111, D06102. doi:10.1029/2005JD006079.
- 1037 Rella, S.F., Tada, R., Nagashima, K., Ikehara, M., Itaki, T., Ohkushi, K., Sakamoto,
1038 T., Harada, N., Uchida, M., 2012. Abrupt changes of intermediate water properties on
1039 the northeastern slope of the Bering Sea during the last glacial and deglacial period.
1040 *Paleoceanography* 27, PA3203. doi:10.1029/2011PA002205.
- 1041 Riethdorf, J.-R., Nürnberg, D., Max, L., Tiedemann, R., Gorbarenko, S.A., Malakhov,
1042 M.I., 2013a. Millennial-scale variability of marine productivity of marine productivity
1043 and terrigenous matter supply in the western Bering Sea over the past 180 kyr. *Clim.*
1044 *Past* 9, 1345-1373. doi:10.5194/cp-9-1345-2013.
- 1045 Riethdorf, J.-R., Max, L., Nürnberg, D., Lembke-Jene, L., Tiedemann, R., 2013b.
1046 Deglacial development of (sub) sea surface temperature and salinity in the subarctic
1047 northwest Pacific: Implications for upper-ocean stratification. *Paleoceanography* 28,
1048 91-104. doi:10.1002/palo.20014.
- 1049 Robinson, R.S., Kienast, M., Albuquerque, A.L., Altabet, M., Contreras, S., De Pol
1050 Holz, R., Dubois, N., Francois, R., Galbraith, E., Hsu, T.-C., Ivanochko, T., Jaccard,
1051 S., Kao, S.-J., Kiefer, T., Kienast, S., Lehmann, M.F., Martinez, P., McCarthy, M.,
1052 Möbius, J., Pedersen, T., Quan, T.M., Ryabenko, E., Schmittner, A., Schneider, R.,
1053 Schneider-Mor, A., Shigemitsu, M., Sinclair, D., Somes, C., Studer, A., Thunell, R.,
1054 Yang, J.-Y., 2012. A review of nitrogen isotopic alteration in marine sediments.
1055 *Paleoceanography* 27, PA4203. doi:10.1029/2012PA002321.
- 1056 Roden, G.I., 1995. Aleutian Basin of the Bering Sea: Thermohaline, oxygen, nutrient,
1057 and current structure in July 1993. *J. Geophys. Res.* 100 (C7), 13539-13554.
1058 doi:10.1029/95JC01291.

- 1059 Roden, G.I., 2000. Flow and water property structures between the Bering Sea and
1060 Fiji in the summer of 1993. *J. Geophys. Res.* 105 (C12), 28595-28612.
1061 doi:10.1029/1999JC000030.
- 1062 Sancetta, C., 1983. Effect of Pleistocene glaciation upon oceanographic
1063 characteristics of the North Pacific Ocean and Bering Sea. *Deep-Sea Res* 30 (8A),
1064 851-869.
- 1065 Sarnthein, M., Statterger, K., Dreger, D., Erlenkeuser, H., Grootes, P., Haupt, B.J.,
1066 Jung, S., Kiefer, T., Kuhnt, W., Pflaumann, U., Schäfer-Neth, C., Schulz, H., Schulz,
1067 M., Seidov, D., Simstich, J., van Kreveld, S., Vogelsang, E., Völker, A., Weinelt, M.,
1068 2001. Fundamental modes and abrupt changes in North Atlantic circulation and
1069 climate over the last 60 ky - Concepts, reconstruction and numerical modeling, in:
1070 Schäfer, P., Ritzrau, W., Schlüter, M., Thiede, J. (Eds.), *The Northern North Atlantic:
1071 A Changing Environment*, Springer, Berlin, pp. 365-410.
- 1072 Schlitzer, R., 2013. Ocean Data View, <http://odv.awi.de> (last access: 4 February
1073 2013).
- 1074 Schlung, S.A., Ravelo, A.C., Aiello, I.W., Andreasen, D.H., Cook, M.S., Drake, M.,
1075 Dyez, K.A., Guilderson, T.P., LaRiviere, J., Stroynowski, Z., Takahashi, K., 2013.
1076 Millennial-scale climate change and intermediate water circulation in the Bering Sea
1077 from 90 ka: A high-resolution record from IODP Site U1340. *Paleoceanography* 28,
1078 1-14. doi:10.1029/2012PA002365.
- 1079 Seki, O., Ikehara, M., Kawamura, K., Nakatsuka, T., Ohnishi, K., Wakatsuchi, M.,
1080 Narita, H., Sakamoto, T., 2004. Reconstruction of paleoproductivity in the Sea of
1081 Okhotsk over the last 30 kyr. *Paleoceanography* 19, PA1016.
1082 doi:10.1029/2002PA000808.
- 1083 Shigemitsu, M., Narita, H., Watanabe, Y.W., Harada, N., Tsunogai, S., 2007. Ba, Si,
1084 U, Al, Sc, La, Th, C and $^{13}\text{C}/^{12}\text{C}$ in a sediment core in the western subarctic Pacific
1085 as proxies of past biological production. *Mar. Chem.* 106, 442-455.
1086 doi:10.1016/j.marchem.2007.04.004.

- 1087 Shigemitsu, M., Watanabe, Y.W., Narita, H., 2008. Time variations of $\delta^{15}\text{N}$ of organic
1088 nitrogen in deep western subarctic Pacific sediment over the last 145 ka. *Geochem.*
1089 *Geophys. Geosy.* 9 (10), Q10012. doi:10.1029/2008GC001999.
- 1090 Sigman, D.M., Altabet, M.A., McCorkle, D.C., Francois, R., Fischer, G., 1999. The
1091 $\delta^{15}\text{N}$ of nitrate in the Southern Ocean: Consumption of nitrate in surface waters.
1092 *Global Biogeochem. Cy.* 13 (4), 1149-1166. doi:10.1029/1999GB900038.
- 1093 Sigman, D.M., Altabet, M.A., McCorkle, D.C., Francois, R., Fischer, G., 2000. The
1094 $\delta^{15}\text{N}$ of nitrate in the Southern Ocean: Nitrogen cycling and circulation in the ocean
1095 interior. *J. Geophys. Res.* 105 (C8), 19599-19614.
- 1096 Sigman, D.M., Lehman, S.J., Oppo, D.W., 2003. Evaluating mechanisms of nutrient
1097 depletion and ^{13}C enrichment in the intermediate-depth Atlantic during the last ice
1098 age. *Paleoceanography* 18 (3), 1072. doi:10.1029/2002PA000818.
- 1099 Sigman, D.M., Hain, M.P., Haug, G.H., 2010. The polar ocean and glacial cycles in
1100 atmospheric CO_2 concentration. *Nature* 466, 47-55. doi:10.1038/nature09149.
- 1101 Smith, S.L., Henrichs, S.M., Rho, T., 2002. Stable C and N isotopic composition of
1102 sinking particles and zooplankton over the southeastern Bering Sea shelf. *Deep-Sea*
1103 *Res. Pt. II* 49, 6031-6050. doi:10.1016/S0967-0645(02)00332-6.
- 1104 Somes, C.J., Schmittner, A., Galbraith, E.D., Lehmann, M.F., Altabet, M.A., Montoya,
1105 J.P., Letelier, R.M., Mix, A.C., Bourbonnais, A., Eby, M., 2010. Simulating the global
1106 distribution of nitrogen isotopes in the ocean. *Global Biogeochem. Cy.* 24, GB4019.
1107 doi:10.1029/2009GB003767.
- 1108 Springer, A.M., McRoy, C.P., Flint, M.V., 1996. The Bering Sea Green Belt: Shelf-
1109 edge processes and ecosystem production. *Fish. Oceanogr.* 5, 205-223.
- 1110 Stabeno, P.J., Schumacher, J.D., Ohtani, K., 1999. The physical oceanography of
1111 the Bering Sea, in: Loughlin, T.R., Ohtani, K. (Eds.), *Dynamics of the Bering Sea*.
1112 University of Alaska Sea Grant, Fairbanks, Alaska, pp. 1-28.
- 1113 Takahashi, K., Fujitani, N., Yanada, M., 2002a. Long term monitoring of particle
1114 fluxes in the Bering Sea and the central subarctic Pacific Ocean, 1990-2000. *Progr.*
1115 *Oceanogr.* 55, 95-112. doi:10.1016/S0079-6611(02)00072-1.

- 1116 Takahashi, T., Sutherland, S.C., Sweeney, C., Poisson, A., Metzl, N., Tilbrook, B.,
1117 Bates, N., Wanninkhof, R., Feely, R.A., Sabine, C., Olafsson, J., Nojiri, Y., 2002b.
1118 Global sea-air CO₂ flux based on climatological surface ocean pCO₂, and seasonal
1119 biological and temperature effects. *Deep-Sea Res.* Pt. II 49, 1601-1622.
1120 doi:10.1016/S0967-0645(02)00003-6.
- 1121 Tanaka, S., Takahashi, K., 2005. Late Quaternary paleoceanographic changes in the
1122 Bering Sea and the western subarctic Pacific based on radiolarian assemblages.
1123 *Deep-Sea Res.* Pt. II 52, 2131-2149. doi:10.1016/j.dsr2.2005.07.002.
- 1124 Ternois, Y., Kawamura, K., Keigwin, L., Ohkouchi, N., Nakatsuka, T., 2001. A
1125 biomarker approach for assessing marine and terrigenous inputs to the sediments of
1126 Sea of Okhotsk for the last 27,000 years. *Geochim. Cosmochim. Ac.* 65 (5), 791-802.
- 1127 Thunell, R.C., Sigman, D.M., Muller-Karger, F., Astor, Y., Varela, R., 2004. Nitrogen
1128 isotope dynamics of the Cariaco Basin, Venezuela. *Global Biogeochem. Cy.* 18,
1129 GB3001. doi:10.1029/2003GB002185.
- 1130 Tomczak, M., Godfrey, J.S., 1994. *Regional oceanography: An introduction.* Elsevier
1131 Science Ltd., Oxford, 391 pp.
- 1132 Tsuda, A., Takeda, S., Saito, H., Nishioka, J., Nojiri, Y., Kudo, I., Kiyosawa, H.,
1133 Shiimoto, A., Imai, K., Ono, T., Shimamoto, A., Tsumune, D., Yoshimura, T., Aono,
1134 T., Hinuma, A., Kinugasa, M., Suzuki, K., Sohrin, Y., Noiri, Y., Tani, H., Deguchi, Y.,
1135 Tsurushima, N., Ogawa, H., Fukami, K., Kuma, K., Saino, T., 2003. A mesoscale iron
1136 enrichment in the western subarctic Pacific induces a large centric diatom bloom.
1137 *Science* 300, 958-961. doi:10.1126/science.1082000.
- 1138 Tyrrell, T., Merico, A., Waniek, J.J., Wong, C.S., Metzl, N., Whitney, F., 2005. Effect
1139 of seafloor depth on phytoplankton blooms in high-nitrate, low-chlorophyll (HNLC)
1140 regions. *J. Geophys. Res.* 110, G02007. doi:10.1029/2005JG000041.
- 1141 van Geen, A., Zheng, Y., Bernhard, J.M., Cannariato, K.G., Carriquiry, J., Dean,
1142 W.E., Eakins, B.W., Ortiz, J.D., Pike, J., 2003. On the preservation of laminated
1143 sediments along the western margin of North America. *Paleoceanography* 18 (4),
1144 1098. doi:10.1029/2003PA000911.

- 1145 VanLaningham, S., Pisias, N.G., Duncan, R.A., Clift, P.D., 2009. Glacial-interglacial
1146 sediment transport to the Meiji Drift, northwest Pacific Ocean: Evidence for timing of
1147 Beringian outwashing. *Earth Planet. Sc. Lett.* 277, 64-72.
1148 doi:10.1016/j.epsl.2008.09.033.
- 1149 Waelbroeck, C., Labeyrie, L., Michel, E., Duplessy, J.C., McManus, J.F., Lambeck,
1150 K., Balbon, E., Labracherie, M., 2002. Sea-level and deep water temperature
1151 changes derived from benthic foraminifera isotopic records. *Quaternary Sci. Rev.* 21,
1152 295-305. doi:10.1016/S0277-3791(01)00101-9.
- 1153 Walinsky, S.E., Prah, F.G., Mix, A.C., Finney, B.P., Jaeger, J.M., Rosen, G.P., 2009.
1154 Distribution and composition of organic matter in surface sediments of coastal
1155 Southeast Alaska. *Cont. Shelf Res.* 29, 1565-1579. doi:10.1016/j.csr.2009.04.006.
- 1156 Walsh, E.M., Ingalls, A.E., Keil, R.G., 2008. Sources and transport of terrestrial
1157 organic matter in Vancouver Island fjords and the Vancouver-Washington Margin: A
1158 multiproxy approach using $\delta^{13}\text{C}_{\text{org}}$, lignin phenols, and the ether lipid BIT index.
1159 *Limnol. Oceanogr.* 53 (3), 1054-1063. doi:10.4319/lo.2008.53.3.1054.
- 1160 Wang, Y., Cheng, H., Edwards, R.L., Kong, X., Shao, X., Chen, S., Wu, J., Jiang, X.,
1161 Wang, X., An, Z., 2008. Millennial- and orbital-scale changes in the East Asian
1162 monsoon over the past 224,000 years. *Nature* 451, 1090-1093.
1163 doi:10.1038/nature06692.
- 1164 Warren, B.A., 1983. Why is no deep water formed in the North Pacific? *J. Mar. Res.*
1165 41, 327-347.
- 1166 Waser, N.A.D., Harrison, P.J., Nielsen, B., Calvert, S.E., Turpin, D.H., 1998. Nitrogen
1167 isotope fractionation during the uptake and assimilation of nitrate, nitrite, ammonium,
1168 and urea by a marine diatom. *Limnol. Oceanogr.* 43 (2), 215-224.
- 1169 Yamamoto, M., Tanaka, N., Tsunogai, S., 2001. Okhotsk Sea intermediate water
1170 formation deduced from oxygen isotope systematics. *J. Geophys. Res.* 106 (C12),
1171 31075-31084.
- 1172 Yasuda, I., 1997. The origin of the North Pacific Intermediate Water. *J. Geophys.*
1173 *Res.* 102 (C1), 893-909.

- 1174 Yokoyama, Y., Esat, T.M., 2011. Global climate and sea level: Enduring variability
1175 and rapid fluctuations over the past 150,000 years. *Oceanography* 24 (2), 54-69.
1176 doi:10.5670/oceanog.2011.27.
- 1177 Zhang, J., Woodgate, R., Moritz, R., 2010. Sea ice response to atmospheric and
1178 oceanic forcing in the Bering Sea. *J. Phys. Oceanogr.* 40 (8), 1729-1747.
1179 doi:10.1175/2010JPO4323.1.
- 1180 Zheng, Y., van Geen, A., Anderson, R.F., Gardner, J.V., Dean, W.E., 2000.
1181 Intensification of the northeast Pacific oxygen minimum zone during the Bölling-
1182 Alleröd warm period. *Paleoceanography* 15 (5), 528-536.
- 1183 Ziegler, M., Jilbert, T., de Lange, G.J., Lourens, L.J., and Reichert, G.-J. (2008),
1184 Bromine counts from XRF scanning as an estimate of the marine organic carbon
1185 content of sediment cores, *Geochemistry Geophysics Geosystems*, 9(5), Q05009,
1186 doi:10.1029/2007GC001932.

1187

1188 **Figure captions**

1189 Figure 1: (a) Surface circulation pattern (red arrows; after Tomczak and Godfrey,
1190 1994; Stabeno et al., 1999) and bathymetry of the subarctic North Pacific realm. The
1191 red dot marks the location of sediment core SO201-2-85KL studied here. Published
1192 reference records are marked by yellow dots. Bering Sea: MR06-04-PC24A (Kim et
1193 al., 2011), KH99-3-BOW-8A (Horikawa et al., 2010), HLY02-02-17JPC (Brunelle et
1194 al., 2007, 2010), IODP Site U1340 (Schlung et al., 2013). Okhotsk Sea: YK0712-
1195 GC9A (Khim et al., 2012), GGC27 (Brunelle et al., 2010). NW Pacific: MD01-2416
1196 (Galbraith et al., 2008a), PC13 (Brunelle et al., 2010). NE Pacific: ODP Site 887
1197 (Galbraith et al., 2008a). The modern average maximum sea-ice extent during March
1198 is indicated by the dashed black line (after Niebauer et al., 1999; Zhang et al., 2010;
1199 IRI/LDEO Climate Data Library, <http://iridl.ldeo.columbia.edu/>). Surface currents:
1200 ANSC = Aleutian North Slope Current, BSC = Bering Slope Current, EKC = East
1201 Kamchatka Current, ESC = East Sakhalin Current, NOC = North Okhotsk Current,
1202 SC = Soya Current, WKC = West Kamchatka Current. Straits: bus = Bussol Strait,
1203 kss = Kruzenshtern Strait, ks = Kamchatka Strait, ns = Near Strait, bp = Buldir Pass,
1204 as = Amchitka Strait, ap = Amukta Pass, up = Unimak Pass, bs = Bering Strait. (b)

1205 Surface nitrate concentration during modern summer (July-September; in $\mu\text{mol l}^{-1}$)
1206 from World Ocean Atlas 2009 data (Garcia et al., 2010). Maps produced with "Ocean
1207 Data View" (Schlitzer, 2013).

1208

1209 Figure 2: (a) Relationship between concentrations of total nitrogen (TN) and total
1210 organic carbon (TOC) in samples from core SO201-2-85KL. For the calculation of
1211 molar N/C ratios a linear regression between TOC and TN was used to assess the
1212 fraction of inorganic nitrogen, represented by the intercept of the regression line at
1213 $\text{TOC} = 0$. (b) Comparison with $\delta^{15}\text{N}_{\text{bulk}}$ indicates that there is only a weak linear
1214 relationship between the isotopic signal and TN concentrations ($R^2 = 0.24$; $p < 10^{-4}$).

1215

1216 Figure 3: Linear sedimentation rate (LSR) vs. bulk accumulation rate (AR Bulk), and
1217 comparison of concentration and accumulation rate (AR) records of Siliciclastics,
1218 CaCO_3 , TOC and opal for core SO201-2-85KL.

1219

1220 Figure 4: Records reflecting changes in export production and terrigenous matter
1221 supply in core SO201-2-85KL over the past 180 kyr in comparison with Northern
1222 Hemisphere summer (July-September) insolation at 65°N (after Laskar et al., 2004).
1223 Logging data (underlying grey lines), %Siliciclastics, as well as CaCO_3 and opal
1224 concentrations are from Max et al. (2012) and Riethdorf et al. (2013a, 2013b). Note
1225 inverted axes of %Siliciclastics and XRF Al count rates. The $\delta^{18}\text{O}$ records from the
1226 NGRIP ice core in Greenland (NGRIP members, 2004; GICC05 timescale,
1227 Rasmussen et al., 2006) and from the Sanbao stalagmites in China (Wang et al.,
1228 2008) are shown for reference. Greenland interstadials (GI) are highlighted by pale
1229 red vertical bars. Boundaries of Marine Isotope Stages (MIS) after Lisiecki and
1230 Raymo (2005).

1231

1232 Figure 5: Comparison of $\delta^{13}\text{C}_{\text{bulk}}$ with (a) molar N/C ratios and (b) $\delta^{15}\text{N}_{\text{bulk}}$ for core
1233 SO201-2-85KL. Samples from warm intervals (MIS 5.5, 5.3, 5.1, 3, and 1) are
1234 marked by red dots, while blue dots mark those from cold intervals (MIS 6, 5.4, 5.2,

1235 4, 2), and green triangles indicate Holocene (<11.7 ka BP) samples. Grey-shaded
1236 boxes represent geochemical provenances (after literature data; see text for
1237 references). The dashed lines indicate the applied linear mixing model for the
1238 estimation of m_{terr} . Marine phytoplankton and vascular plant detritus (VPD) are
1239 considered as potential marine and terrestrial organic matter sources (endmembers).

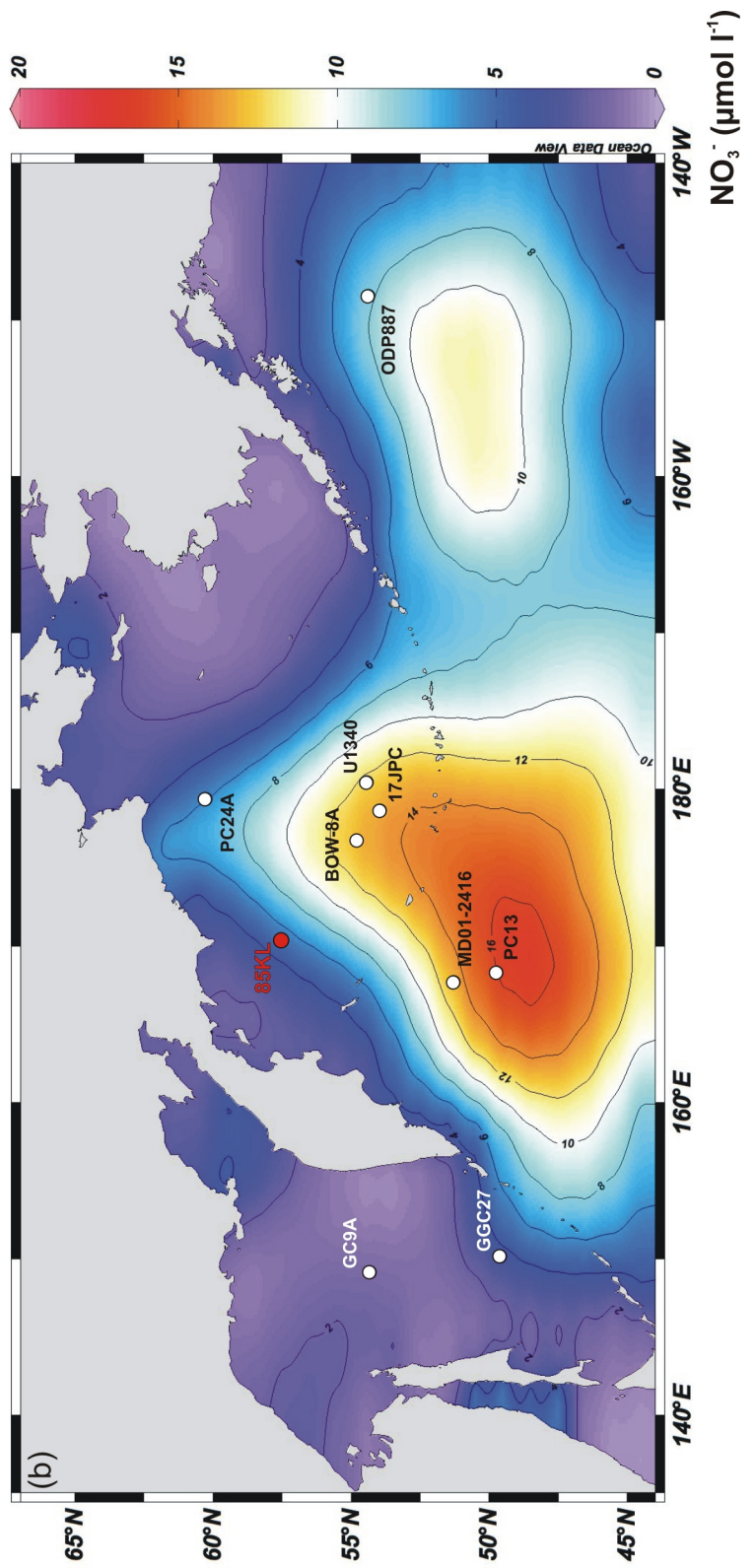
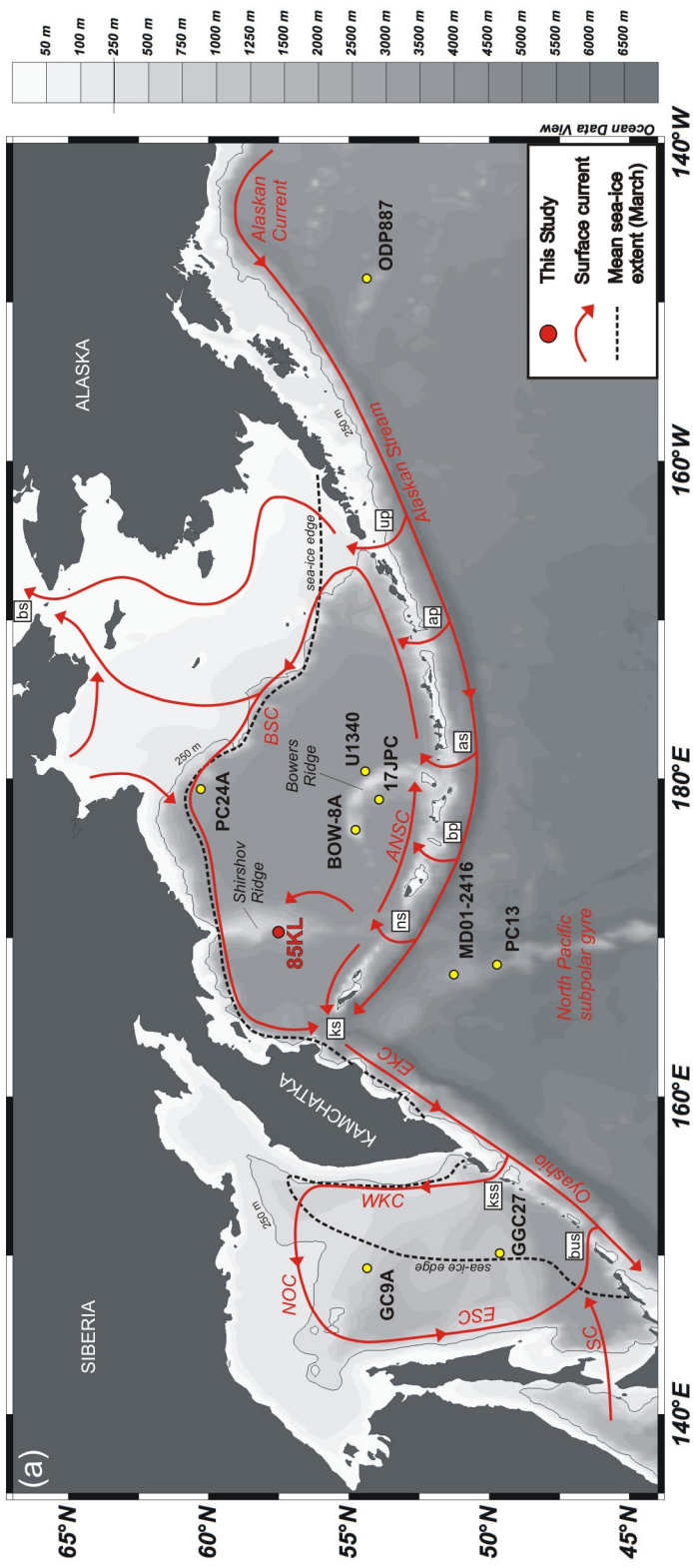
1240

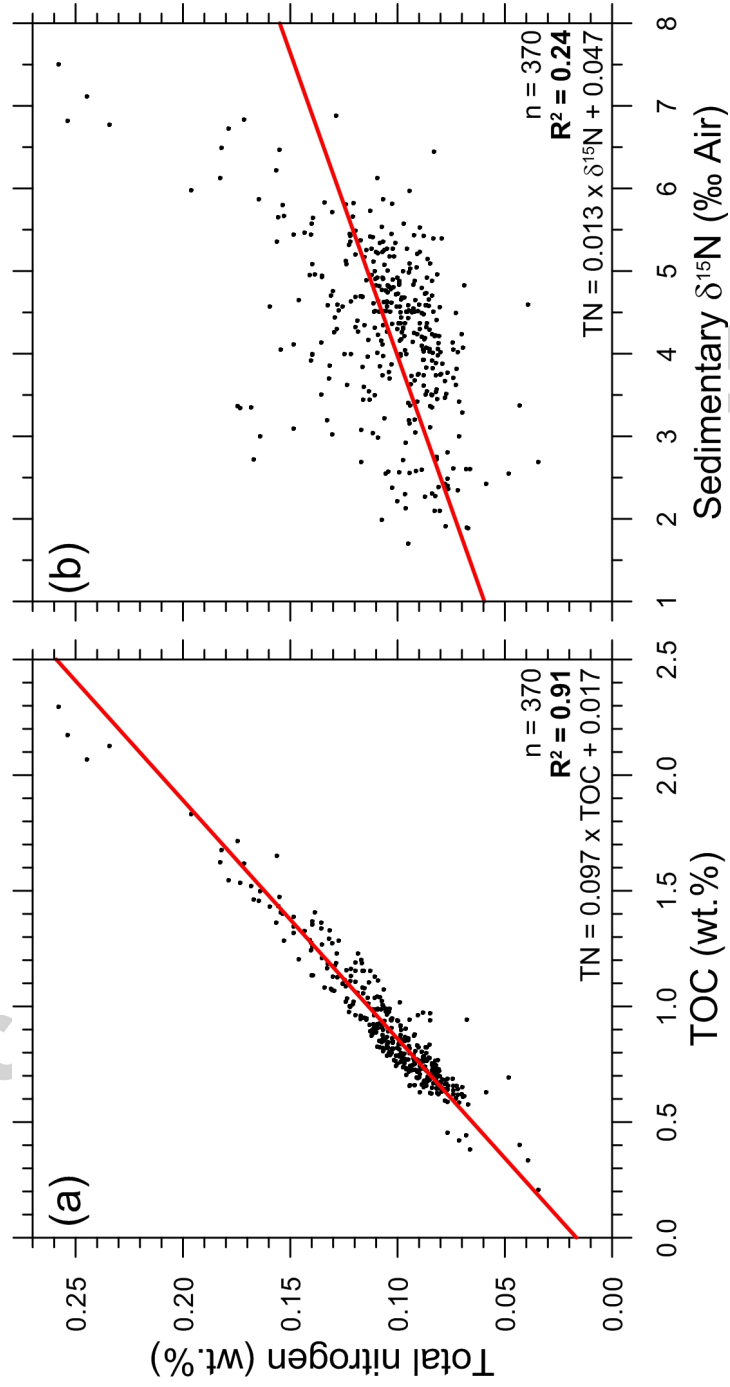
1241 Figure 6: Proxy records from core SO201-2-85KL in comparison with published
1242 reference records covering the last 180 kyr: (a) Northern Hemisphere summer (65°;
1243 July-September) insolation after Laskar et al. (2004), (b) sedimentary $\delta^{13}\text{C}$ and (c)
1244 molar N/C ratios used to estimate the fraction of terrestrial organic matter (m_{terr} ;
1245 respective axes apply to those of $\delta^{13}\text{C}$ and N/C), (d) color b^* assumed to reflect
1246 export production, (e) $\delta^{15}\text{N}_{\text{bulk}}$ reflecting surface nitrate utilization, (f) neodymium
1247 isotope ratios from core KH99-3-BOW-8A (Horikawa et al., 2010; cf. Figure 1)
1248 considered to approximate intermediate water formation, and (g) relative sea-level
1249 (Waelbroeck et al., 2002) normalized to the sill depth (~50 m; dashed line) of the
1250 Bering Strait (ΔRSL). MIS boundaries after Lisiecki and Raymo (2005), GI highlighted
1251 by pale red vertical bars.

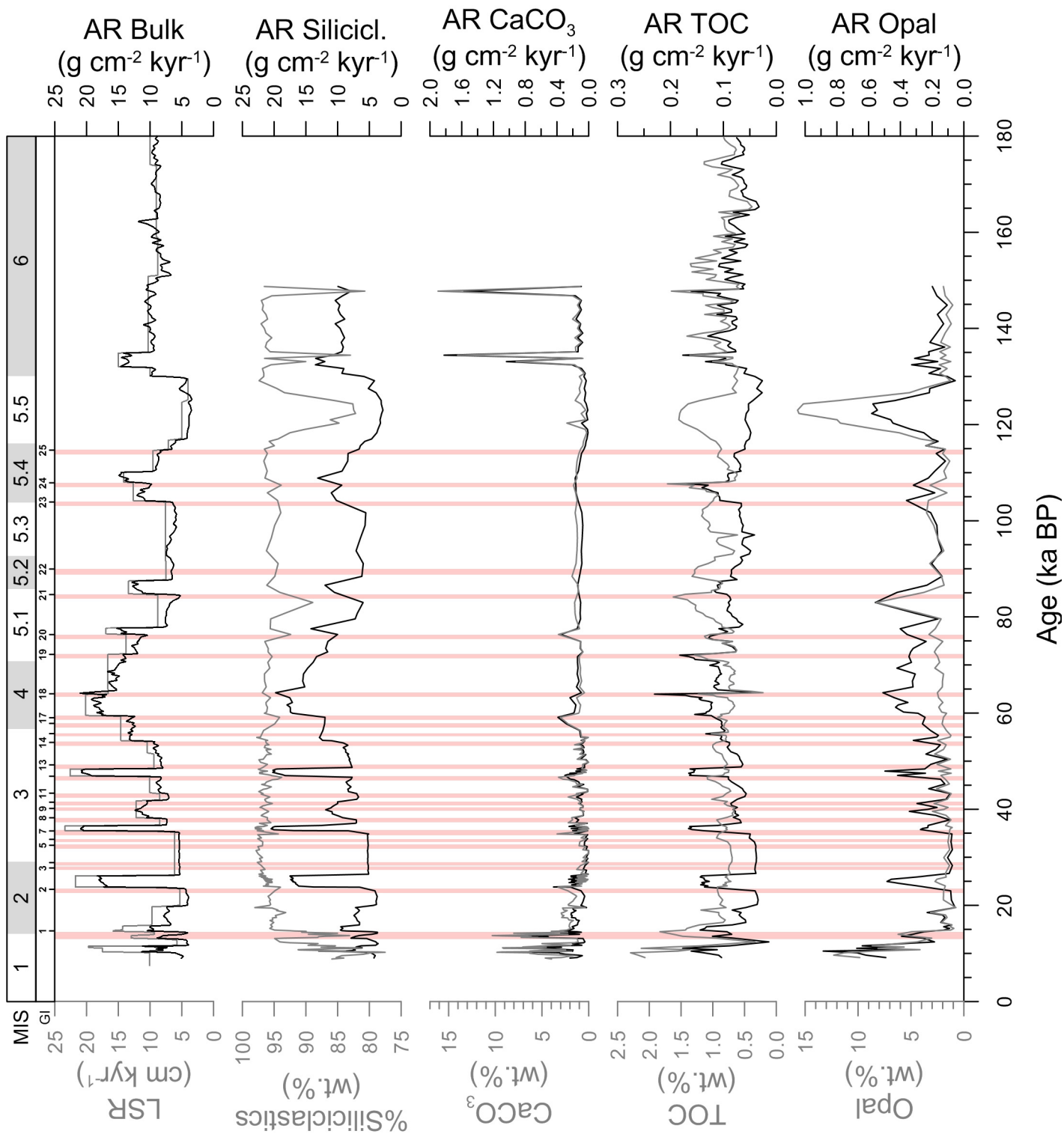
1252

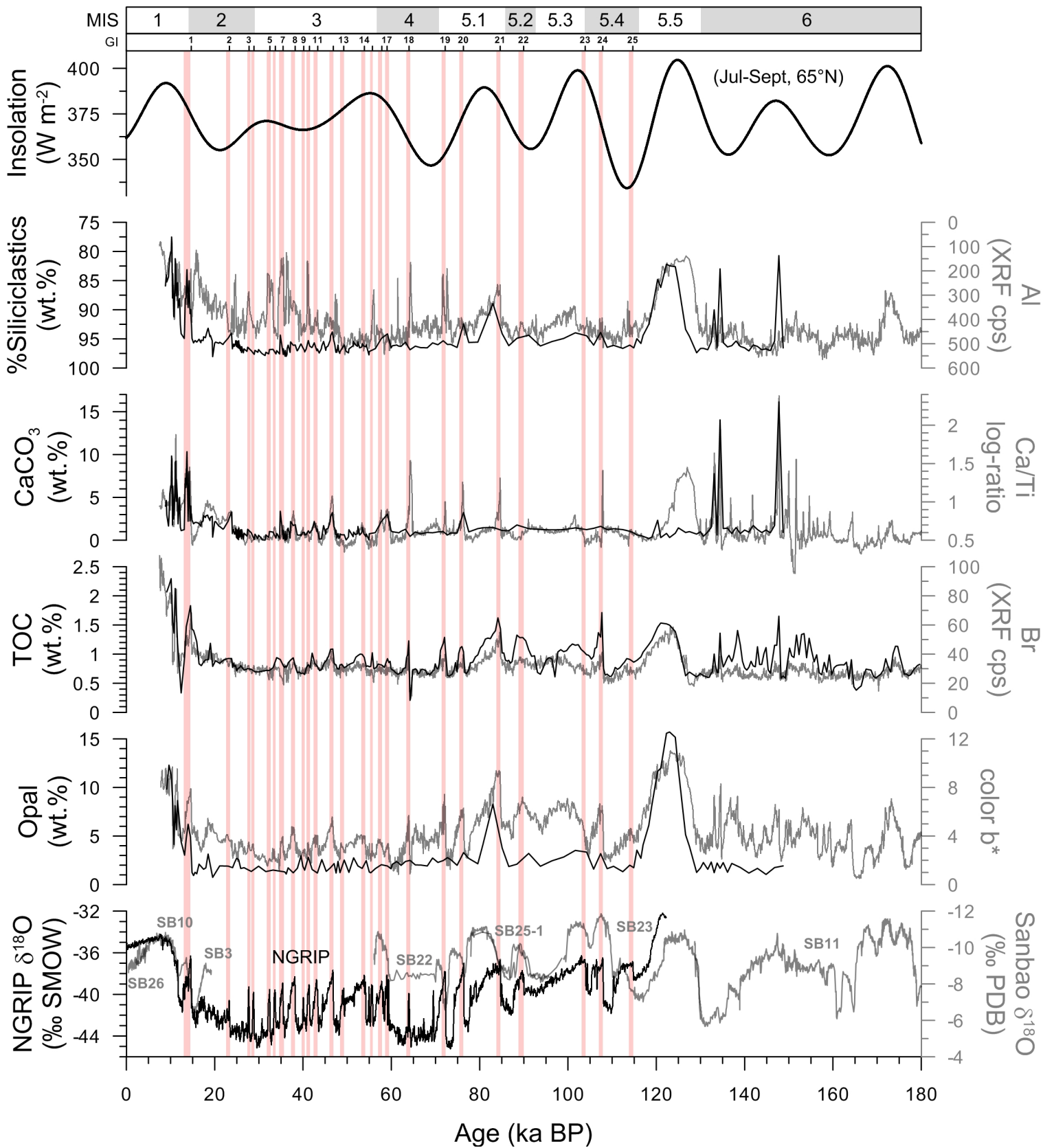
1253 Figure 7: Comparison of $\delta^{15}\text{N}_{\text{bulk}}$ from SO201-2-85KL (black line) with other
1254 sedimentary (solid lines) and diatom-bound (dotted lines) $\delta^{15}\text{N}$ records from the
1255 subarctic North Pacific and its marginal seas (cf. Figure 1). The timing of Greenland
1256 interstadials and MIS boundaries are indicated.

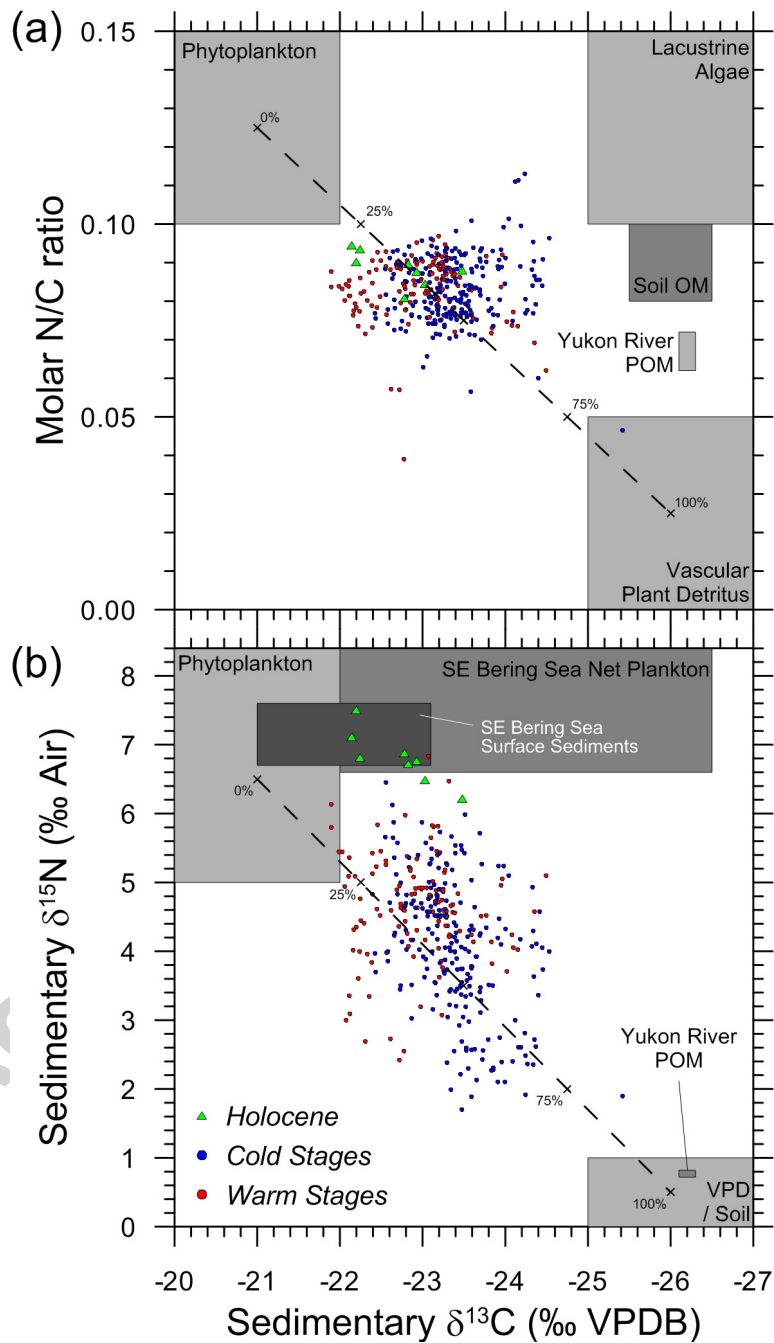
1257

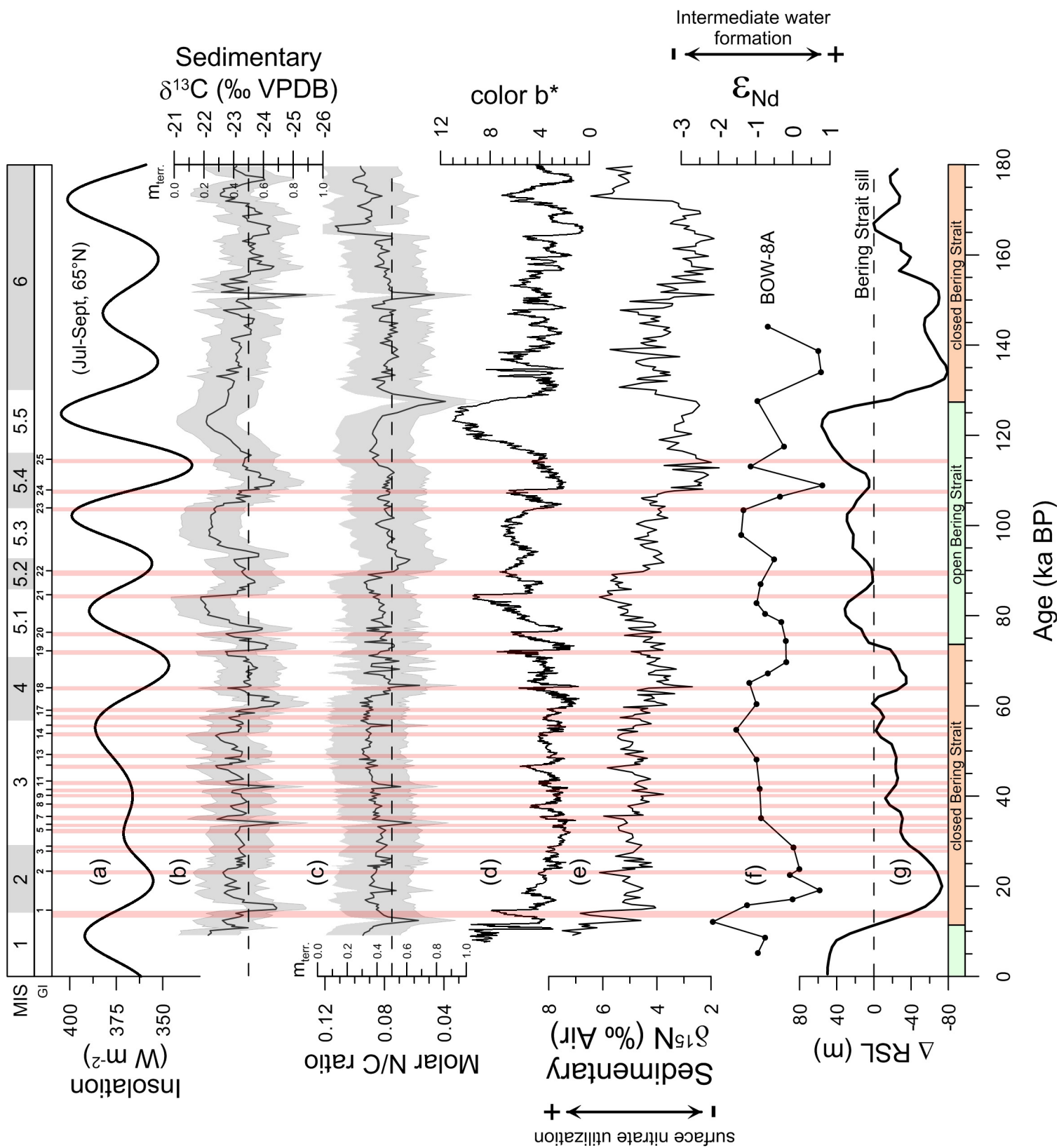












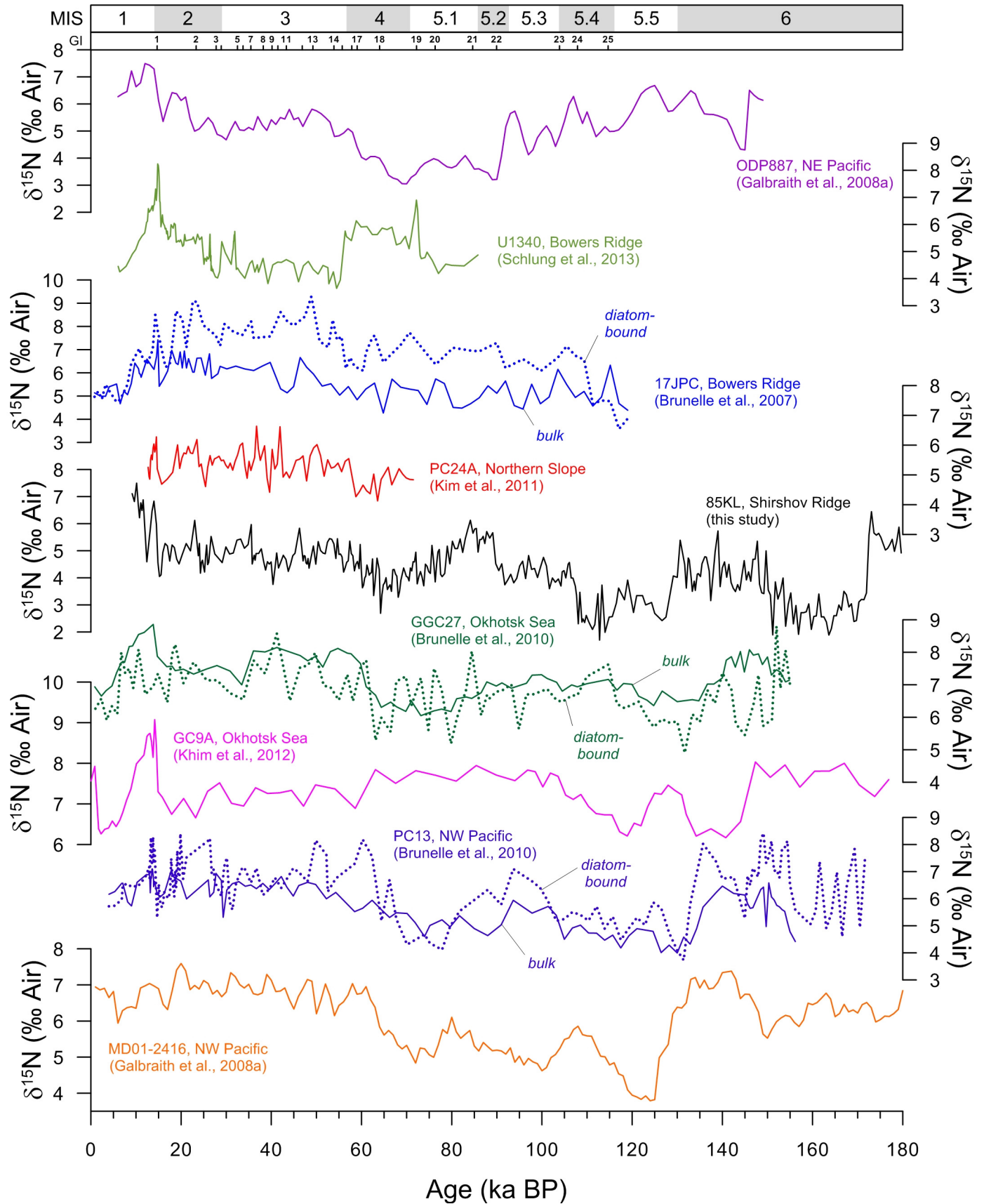


Table 1 Ranges, averages, and variability of $\delta^{13}\text{C}$, molar N/C ratio, and m_{terr} in Core SO201-2-85KL.

Variable	Minimum	Maximum	Average	StDev.
$\delta^{13}\text{C}$ (‰ VPDB)	-25.4	-21.9	-23.2	0.6
molar N/C ratio	0.04	0.11	0.08	0.01
m_{terr} via $\delta^{13}\text{C}$	18%	88%	45%	11%
m_{terr} via N/C	12%	86%	42%	8%

Table 2 Parameters for Calculation of m_{terr} Using Eq. (1).

Variable	Minimum	Maximum	Average
<i>Marine Endmember Composition</i>			
$d^{13}\text{C}_{\text{mar}}$	-20 ‰	-22 ‰	-21‰
$d^{15}\text{N}_{\text{mar}}$	5.0 ‰	/	6.5 ‰
N/C _{mar}	0.100	0.150	0.125
<i>Terrestrial Endmember Composition</i>			
$d^{13}\text{C}_{\text{terr}}$	-25 ‰	-27 ‰	-26 ‰
$d^{15}\text{N}_{\text{terr}}$	0 ‰	1.0 ‰	0.5 ‰
N/C _{terr}	0	0.050	0.025